Controlling Wind Pressure Around Buildings: Using Automated Multi-Angle Ventilation Louvers for Higher Natural Ventilation Potential

Share Your Story

Controlling Wind Pressure Around Buildings:
Using Automated Multi-Angle Ventilation Louvers for Higher Natural Ventilation Potential

By

Sunghwan Lim

Bachelor of Science, Interior Architecture & Built Environment and
Bachelor of Science in Engineering, Architecture & Architectural Engineering, Yonsei University, 2015

Submitted in partial fulfillment of the requirements for the degree of

Master in Design Studies
Energy and Environment Concentration

At the Harvard University Graduate School of Design

May, 2021

Copyright © 2021 by Sunghwan Lim

Signature of the Author _____
Sunghwan Lim
Harvard University Graduate School of Design

Certified by _____
Ali Malkawi
Professor of Architectural Technology
Harvard University Graduate School of Design

Controlling Wind Pressure Around Buildings:

Using Automated Multi-Angle Ventilation Louvers

for Higher Natural Ventilation Potential

Sunghwan Lim

Advisor: Ali Malkawi

May, 2021

ABSTRACT

Natural ventilation (NV) is an effective means of reducing building energy consumption and enhancing indoor air quality (IAQ) by conveying outdoor air into space. Recently, rising concern of climate change and the COVID-19 pandemic arouse interest in utilizing NV. However, the uncertainty of airflow and the complexity of controlling windows that often rely on the occupants prevent achieving higher NV potential. This research proposes an automated multi-angle ventilation louver that can provide a stable airflow into space by controlling the axis position and opening angle, leading to higher NV potential. The performance of the louver was tested on multiple cases of wind condition and louver configurations by computational fluid dynamics (CFD) simulations. The data set collected from the CFD simulations showed that the louver generates higher NV potential compared to the opening without the louvers. Based on the data set, this research introduces a simulation tool developed in Rhinoceros and Grasshopper. The tool assists users in exploring the potential of NV in cases utilizing the louvers at different locations, building programs, and building configurations. The tool further indicates louver control and coordination on an hourly basis that can achieve maximized NV potential. Overall, this research expands the applicability of NV in both new and existing buildings by introducing an automated multi-angle ventilation louver. The louver can be further developed to apply a real-time control system that could accommodate variations of indoor environments and building surrounding conditions.

KEYWORDS

TABLE OF CONTENTS

1. INTRODUCTION

1.1 Motivation and literature review

The United Nations (2018[1]) reported that 55% of the world's population are residing in urban areas in 2018. The ratio is estimated to rise to 68% by the year 2050. The ongoing urbanization will intensify urban heat island effect and climate change, eventually increase energy consumption for cooling the buildings (Santamouris., et al,. 2001[2]; Crawley., 2008[3]).

Natural ventilation (NV) has been considered one of the most effective energy-saving strategies to reduce the energy required for cooling, enhance thermal comfort, and improve indoor air quality (IAQ) (Luo., et al,. 2007[4]; Tong ., et al,. 2007[5], Korsavi., et al,. 2020[6]). The term NV potential is frequently studied to quantify the availability of NV or potential to reduce the energy required for cooling and ventilating buildings (Aynsley 1999[7];Yao., et al,. 2009[8]; Cheng., et al,.

---

[1] UN, World Urbanization Prospects: The 2018 Revision, Department of Economic and Social Affairs, United Nations, 2018.

[2] Santamouris, M., Papanikolaou, N., Livada, I., Koronakis, I., Georgakis, C., Argiriou, A., & Assimakopoulos, D. N. (2001). On the impact of urban climate on the energy consumption of buildings. *Solar energy*, *70*(3), 201-216.

[3] Crawley, D. B. (2008). Estimating the impacts of climate change and urbanization on building performance. *Journal of Building Performance Simulation*, *1*(2), 91-115.

[4] Luo, Z., Zhao, J., Gao, J., & He, L. (2007). Estimating natural-ventilation potential considering both thermal comfort and IAQ issues. *Building and environment*, *42*(6), 2289-2298.

[5] Tong, Z., Chen, Y., Malkawi, A., Liu, Z., & Freeman, R. B. (2016). Energy saving potential of natural ventilation in China: The impact of ambient air pollution. *Applied energy*, *179*, 660-668.

[6] Korsavi, S. S., Montazami, A., & Mumovic, D. (2020). Indoor air quality (IAQ) in naturally-ventilated primary schools in the UK: occupant-related factors. *Building and Environment*, *180*, 106992.

[7] Aynsley, R. (1999). Estimating summer wind driven natural ventilation potential for indoor thermal comfort. *Journal of Wind Engineering and Industrial Aerodynamics*, *83*(1-3), 515-525.

[8] Yao, R., Li, B., Steemers, K., & Short, A. (2009). Assessing the natural ventilation cooling potential of office buildings in different climate zones in China. *Renewable Energy*, *34*(12), 2697-2705.

2018[9]; Sakiyama., et al,. 2021[10]). Among the studies those defined NV potentials, Chen, Tong,

and Malkawi (2016[11]) investigated NV potential in various cities worldwide by defining the NV

hour, which is an indicator to measure the natural ventilation potentials in time scale. To

determine whether a specific hour is a NV hour or not, ASHRAE -55 Adaptive Comfort

Standard was employed and conditions in Eqn. (1) were defined. If the outdoor temperature at a

certain hour falls between T_{up} and T_{low}, and T_{dew} is lower than 17°C, that hour is NV hour.

$$T_{up} = 0.31T_{out} + 17.8 + \frac{1}{2}\Delta T_{80\%} \tag{1}$$

$$T_{low} = 12.8°C$$

$$T_{dew} < 17°C$$

Where T_{out} is the monthly average outdoor temperature and $\Delta T_{80\%}$ is 80% acceptability

temperature band in the adaptive comfort chart. Stepping further from the NV hour definition,

the ongoing research at the Harvard Center for Green Building and Cities subcategorized NV

hour into regional NV hour and spatial NV hour. Regional NV hour is the same as the

conventional way to calculate NV hour with localized weather conditions. On the other hand,

spatial NV hour considers the effect of wind condition, window type, effective opening areas,

and building orientation to calculate outdoor airflow into space. Though a specific hour is

regional NV hour, if the calculated airflow is insufficient for cooling space and maintaining IAQ

---

[9] Cheng, J., Qi, D., Katal, A., Wang, L. L., & Stathopoulos, T. (2018). Evaluating wind-driven natural ventilation potential for early building design. *Journal of Wind Engineering and Industrial Aerodynamics*, *182*, 160-169.

[10] Sakiyama, N. R. M., Mazzaferro, L., Carlo, J. C., Bejat, T., & Garrecht, H. (2021). Natural ventilation potential from weather analyses and building simulation. *Energy and Buildings*, *231*, 110596

[11] Chen, Y., Tong, Z., & Malkawi, A. (2017). Investigating natural ventilation potentials across the globe: Regional and climatic variations. *Building and Environment*, *122*, 386-396.

of space, that hour is not defined as a spatial NV hour. The diagram of defining spatial NV hour

is shown in Figure 1. The concept of regional NV hour and spatial NV hour will be employed in

this research to analyze the NV potential of a given region or space.
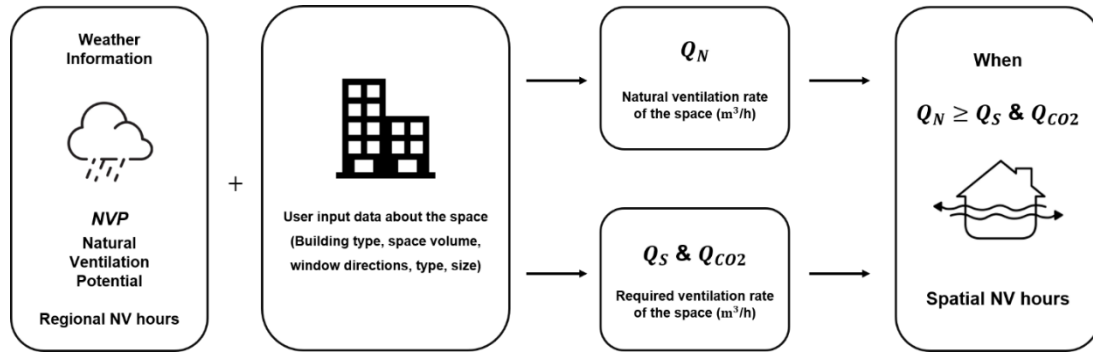

Figure 1: Diagram of defining spatial NV hour

Many researchers have studied to increase NV potential. Wang and Malkawi (2015[12]) proposed a

genetic algorithm based building form optimization methodology to bring higher NV potential.

The CFD simulation program evaluates pressure distribution on the building façade considering

the surrounding environment and the genetic algorithm output NV optimized building design for

designers in the early design stages. Some researchers studied the window types and window

location for higher NV potential. Lim and Kim (2017[13]) have concluded that the operable

windows should be installed at the upper part of the wall for better ventilation, and the maximum

projection angle of a top-hung window should be increased from 20° to 30° to meet the required

ventilation rate. Yoon, Piette, Han, Wu, and Malkawi (2020[14]) applied CFD simulation results to

---

[12] Wang, B., & Malkawi, A. (2015). Genetic algorithm based building form optimization study for natural ventilation potential. In *BS2015: 14th Conference of International Building Performance Simulation Association*.

[13] Lim, H. S., & Kim, G. (2018). The renovation of window mechanism for natural ventilation in a high-rise residential building. *International Journal of Ventilation*, *17*(1), 17-30.

[14] Yoon, N., Piette, M. A., Han, J. M., Wu, W., & Malkawi, A. (2020). Optimization of Wind Positions for Wind-Driven Natural Ventilation Performance. *Energies*, *13*(10), 2464.

find the optimized window positions for wind-driven natural ventilation performance. In this research, higher NV potential will be accomplished by providing stable airflow that satisfies outdoor air demand for cooling and ventilating.

When the wind travels around the building, different amount pressure is distributed around a building as shown in Figure 2.
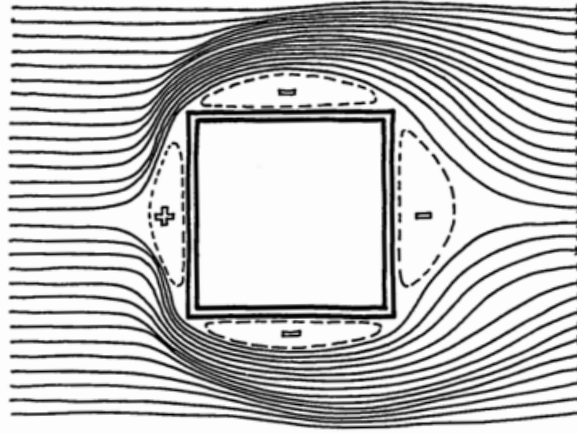
Figure 2: Relative wind pressure schematic around a building[15]

The pressure difference on a building surface is one of the main drivers for NV. The airflow rate (m^3/s) between two openings is proportional to the square root of pressure difference and can be expressed as Eqn. (2) which is the simplified equation of standard orifice flow equation.

$$Q = C_d A_{eff} v \sqrt{C_{pi} - C_{po}} \tag{2}$$

Where C_d is discharge coefficient of an opening, A_{eff} is an effective area, v is wind velocity, C_{pi} is pressure coefficient at inlet, C_{po} is pressure coefficient at outlet. Conventional windows can

---

[15] Moere, Fuller. *Environmental Control Systems: Heating, Cooling, Lighting.* McGraw-Hill College, 1992.

control the flow area by opening and closing but do not effectively control the pressure difference across openings to manipulate the airflow. The case in Figure 3 shows the obstacles near the openings forming wind pressure difference and introducing airflow into space. If there were no obstacles, the wind blowing from the left corner of the building would create the same pressure coefficient on the openings, and only small airflow will be introduced into space.
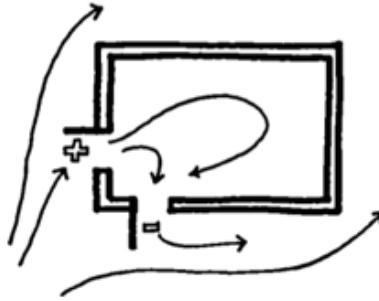
Figure 3: Forming wind pressure difference between the openings by obstacles [16]

Many researchers attempted to increase NV potential in a similar concept. Chiang, Chen, Chou, Li, and Lien (2005[17]) studied the influence of horizontal louvers on NV in a dwelling unit. They have found that the louver with a fixed angle of 120° increased the amount of air change along with the depth of louvers. Scheuring and Weller (2020[18]) proposed an automated self-sufficient façade system that can generate energy by an integrated photovoltaic panel and uses NV to control indoor air climate. The horizontal fins in the system open up to 80° and allow airflow needed in the space for indoor air quality. In research conducted by Yang, Kim, Song, Choi, and

---

[16] Moere, Fuller. Environmental Control Systems: Heating, Cooling, Lighting. McGraw-Hill College, 1992.

[17] Chiang, C., Chen, N., Chou, P., Li, Y., & Lien, I. (2005, September). A study on the influence of horizontal louvers on natural ventilation in a dwelling unit. In *Proceeding of the 10th International Conference on Indoor Air Quality and Climate* (pp. 4-9).

[18] Scheuring, L., & Weller, B. (2020). Natural ventilation provided by a self-sufficient facade system. In *IOP Conference Series: Earth and Environmental Science* (Vol. 410, No. 1, p. 012116). IOP Publishing.

Park (2020[19]), windcatcher louvers are designed to capture air flowing outside a building to increase its NV. They have adopted the design of the Clark Y airfoil to increase the ventilation rate.

However, a fixed device cannot promise the constant airflow that space demands while the wind condition changes. The limitation on a fixed device can be overcome by designing a multi-angle louver that can displace according to the weather condition.

Another way to gain higher NV potential is by designing a control system automating the control of the window openings. In most of the buildings, NV relies on the occupant control of opening and closing a window. However, occupant controlled ventilation is influenced by a variety of parameters and can lowers the potential of utilizing NV. Research on user behavior regarding ventilation by Fritsch, Kohler, Nygard-Ferguson, and Scartezzini (1990[20]) found from their field study that the occurrence of an open window and the opening angle was independent of the ambient temperature during the summer season. Yun, Steemers, and Baker (2008[21]) concluded that building and façade design has a large impact on occupant's perceived comfort and controllability over their environment. Research conducted by Chen, Tong, Samuelson, Wu, and Malkawi (2018[22]) compared the energy performance and thermal comfort of a building using three main types of window control schemes. Those are spontaneous occupant control, informed

[19] Yang, Y. K., Kim, M. Y., Song, Y. W., Choi, S. H., & Park, J. C. (2020). Windcatcher Louvers to Improve Ventilation Efficiency. *Energies*, *13*(17), 4459.

[20] Fritsch, R., Kohler, A., Nygård-Ferguson, M., & Scartezzini, J. L. (1990). A stochastic model of user behaviour regarding ventilation. *Building and Environment*, *25*(2), 173-181.

[21] Yun, G. Y., Steemers, K., & Baker, N. (2008). Natural ventilation in practice: linking facade design, thermal performance, occupant perception and control. *Building Research & Information*, *36*(6), 608-624.

[22] Chen, Y., Tong, Z., Samuelson, H., Wu, W., & Malkawi, A. (2019). Realizing natural ventilation potential through window control: the impact of occupant behavior. *Energy Procedia*, *158*, 3215-3221.

occupant control, and fully automatic control. It was found that informed occupant control recorded the highest discomfort hours and fully automatic control achieved the highest energy saving.

1.2 Objectives

The main objective of this research is to increase NV potential in a building to decrease energy consumption from heating, ventilating, and air conditioning (HVAC) systems and improve IAQ by introducing more outdoor air in space. This will be accomplished by providing stable airflow that satisfies outdoor air demand for cooling and ventilating. An automated control system will control the louvers that can manipulate wind pressure around the openings and opening area. Consequently, NV potential will increase by accepting NV from an extended range of wind speed and directions. The louvers and their control system will be adapted to the conventional buildings that were not feasible to utilize NV and applied for the new buildings to achieve higher energy efficiency.

2. METHODOLOGY

2.1 Louver design

The objective of the louver design is to control the pressure at the inlet and outlet of air and to change the opening area at the same time with a minimum amount of hardware. Figure 4 shows the louver design for a space where cross ventilation is available. For cross ventilation, two or more louvers will be placed at the exterior walls. One will be an inlet of air creating relatively positive pressure, and the others will be an outlet of air creating relatively negative pressure.

Figure 4: Design of the louver for cross ventilation

Next, Figure 5 shows the louver design for space where only single-sided ventilation is available. For single-sided ventilation, a single louver will be placed at the exterior wall. There are two outer panels placed vertically. One will be an inlet of air creating relatively positive pressure, and another panel will be an outlet of air creating relatively negative pressure.
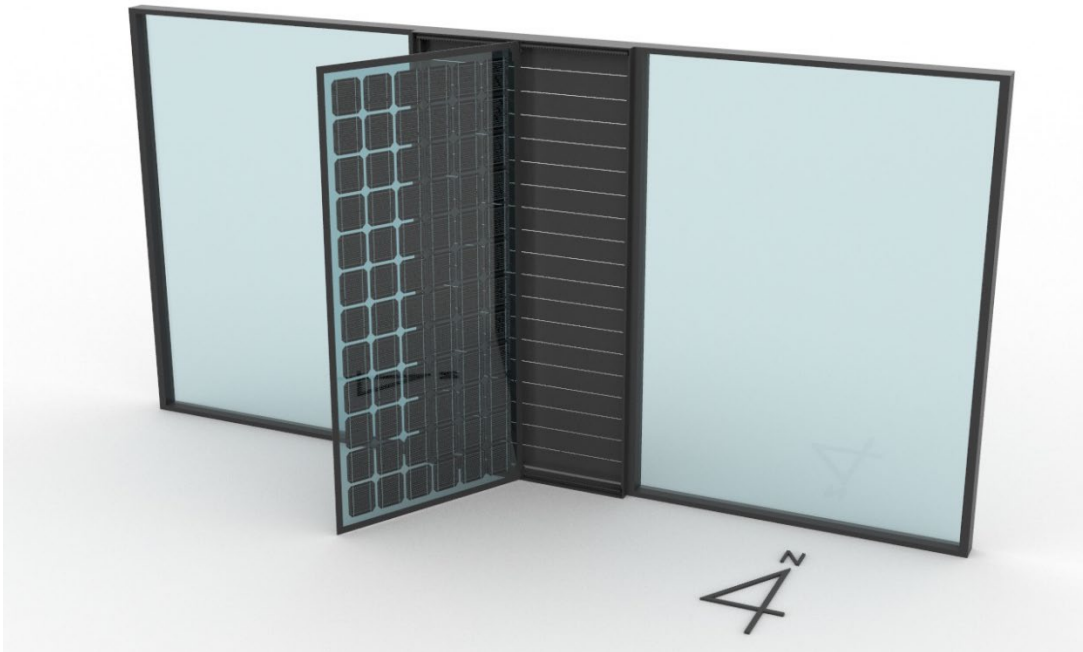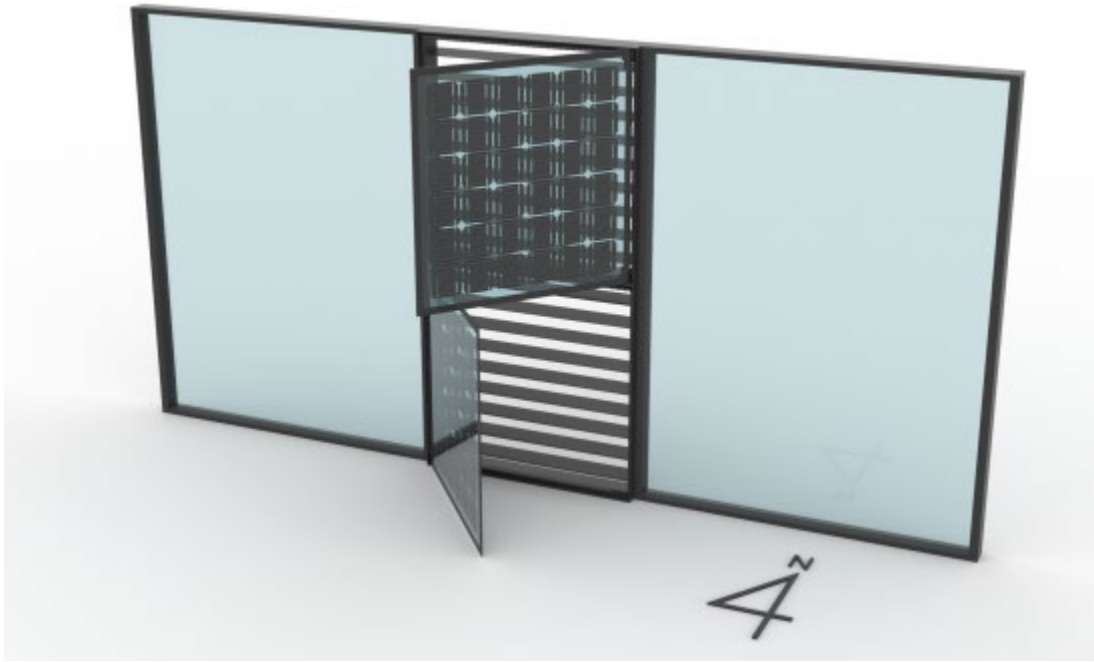
Figure 5: Design of the louver for sing-sided ventilation

2.1.1 Specification

The size of the louver is W x H = 1 x 2 m, and it is designed to be a segment in the curtain wall system consisting of the inner fins and the outer panel. The inner fins are designed to completely close the louver or open and induce incoming air upward or downward. The outer panel is consisted with metal frame and bifacial photovoltaic panel. As shown in Figure 6, there two motor modules at the top and the bottom between the outer panel and the mainframe. Motor modules receive a command from the main controller, control the outer panel's opening angle, move the outer panel horizontally. The gears located at the top and bottom carry the outer panel following the tracks mounted.
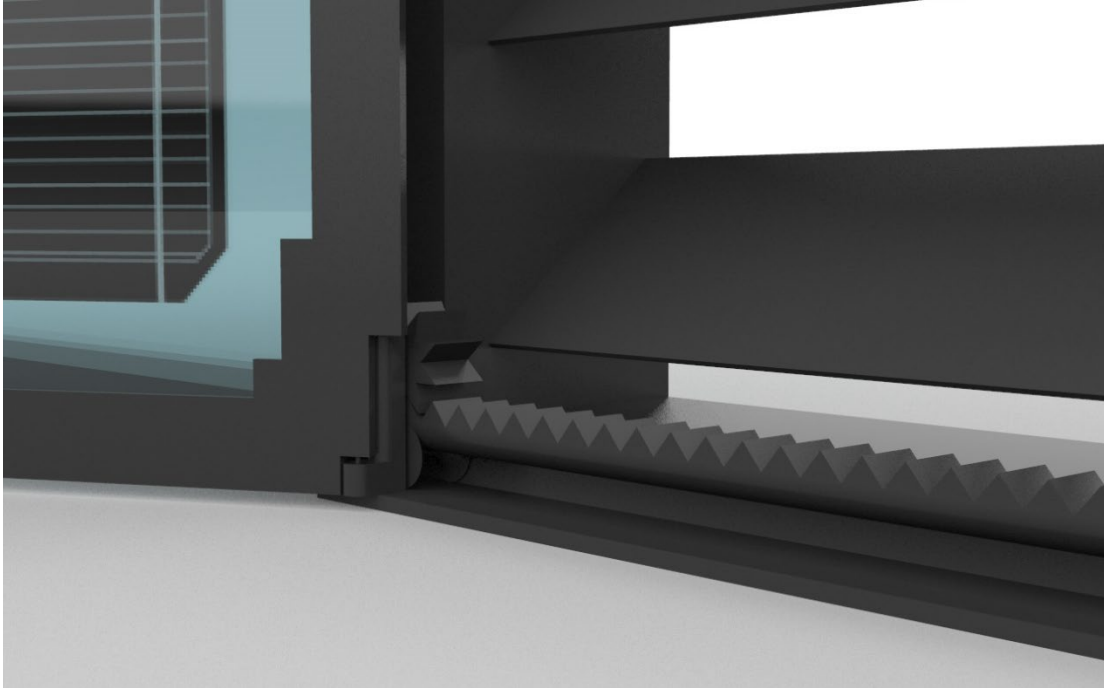
Figure 6: The louver motor module, gear, and track

2.1.2 Operating mechanism

When NV is available, the louver operates in the NV mode. In the NV mode, the louver is controlled to received demanded airflow for cooling and ventilating a space. Figure 7 shows the outer panel placement according to the two wind conditions. When the wind blows from the west, the outer panel is located at the right side of the louver and opened to a certain degree angle to form relatively positive pressure and adequate opening area. When the wind blows from the east, the outer panel is located at the right side of the louver and opened to a certain degree angle to form relatively positive pressure and adequate opening area. During the NV mode, energy is

produced at the mounted photovoltaic panel.
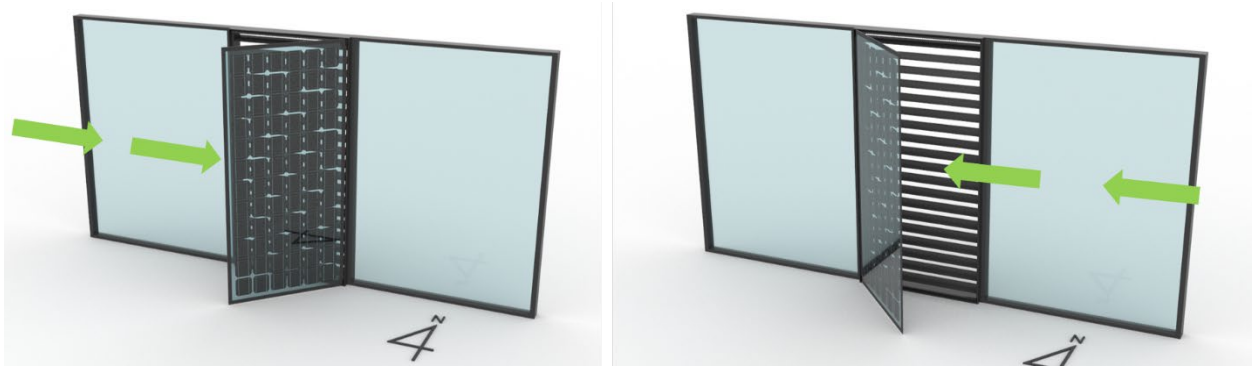
Figure 7: Outer panel movement according to the wind conditions (west wind-left, east wind-right)

When NV is not available, the louver operates in the PV mode. The outer panel is controlled for the photovoltaic panel to produce a maximum amount of energy. Accordingly, the outer panel is opened to an angle perpendicular to the sun's azimuth. On the other hand, the inner fins are opened at an angle that can intake a minimum amount of outdoor air required to maintain IAQ of the space.
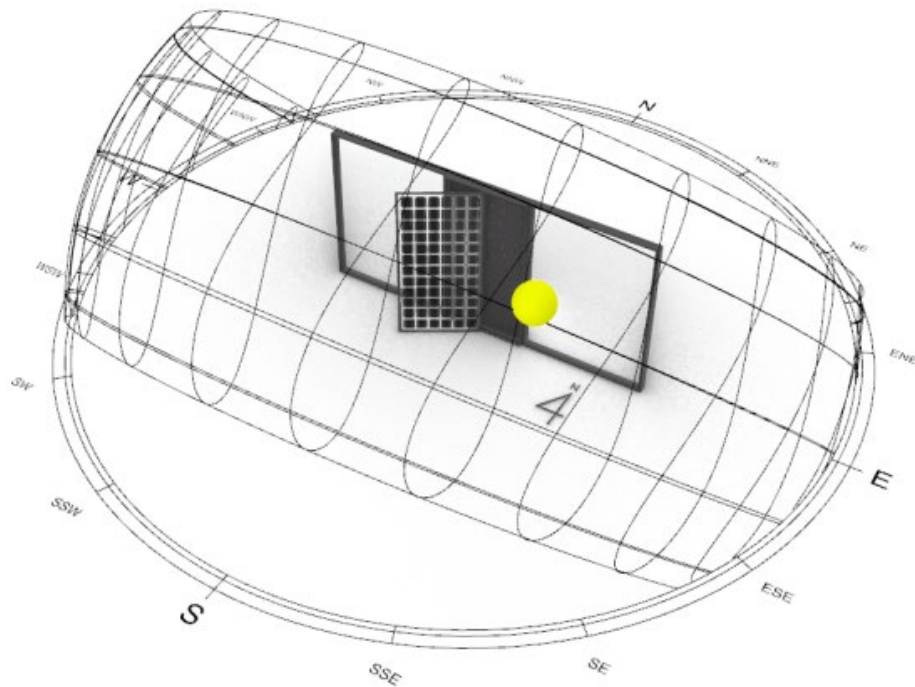
Figure 8: The louver operation during non-NV season

2.2 Louver performance analysis

The louver performance was tested by measuring airflow passing through the openings. The control group is an opening without the louvers, and the experimental group is an opening with the louvers, as shown in Figure 9. The airflow of each group was tested by CFD simulation software FloVENT 11.1.
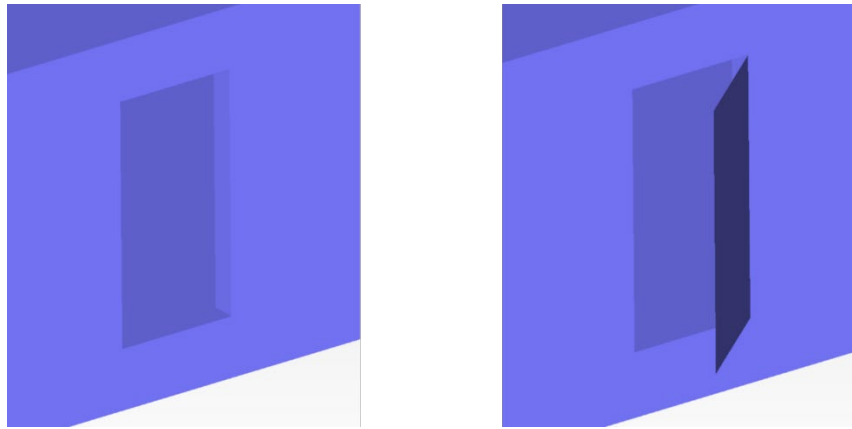
Figure 9: Opening groups (control group-left, experimental group-right)

2.2.1 CFD simulation model description

In the model setup, the type of solution was set to flow only. K-epsilon model was employed for turbulence model, which is the most common model used CFD to simulate mean flow characteristics for turbulent flow conditions. The air temperature was set to 20 with 50% relative humidity.

The CFD domain size is L x W x H = 30 x 30 x 10 m as in Figure 10. The CFD domain needs to follow the blockage ratio that avoids artificial acceleration by non-physical boundaries. However, considering the time required for each round of CFD simulation and after testing that

airflow was negligibly impacted by reduced domain size, the domain size was reduced to 30 x 30 x 10 m. The target space is located at the center of the domain, and the size is L x W x H = 10 x 10 x 3 m. Openings are placed at the center of the wall, and each size is W x H = 1 x 2 m.
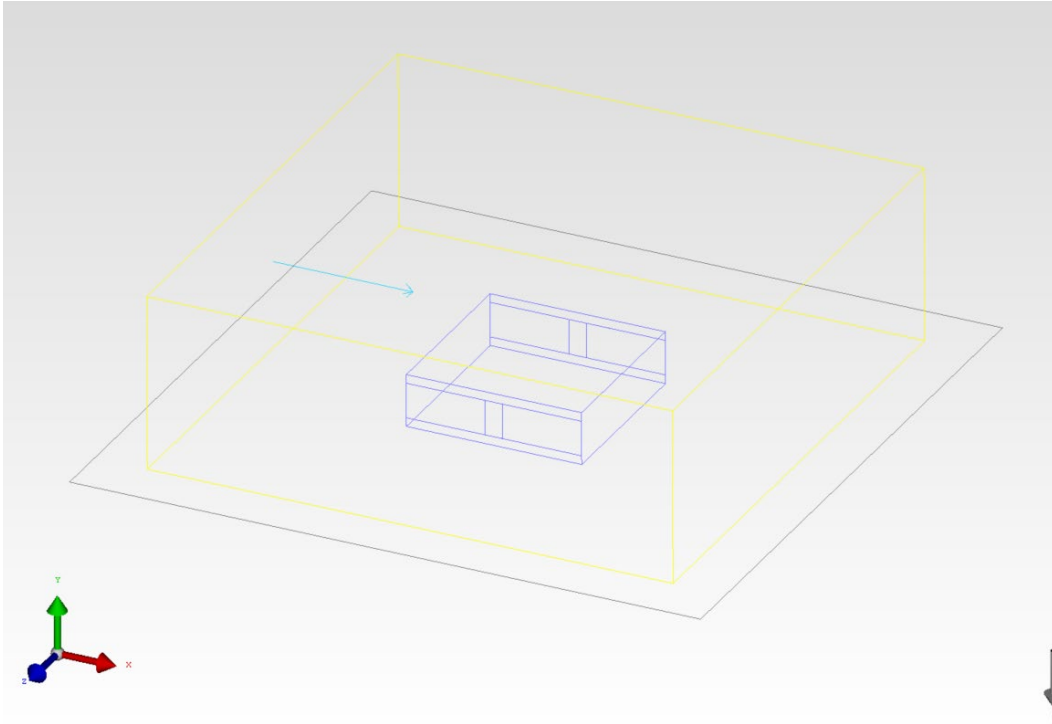
Figure 10: CFD simulation domain

The total cell number is approximately 357,840, and the grids are more refined near the openings and the louvers for high accuracy in airflow calculation. In specific, Figure 11 shows standard cell size is L x W x H = 50 x 50 x 50 cm in the domain, and cell size is reduced to L x W x H = 5 x 5 x 5 around the openings. The cell sizes were determined based on the tests that airflow remained constant in certain cell sizes and the time required for each round of CFD simulation.
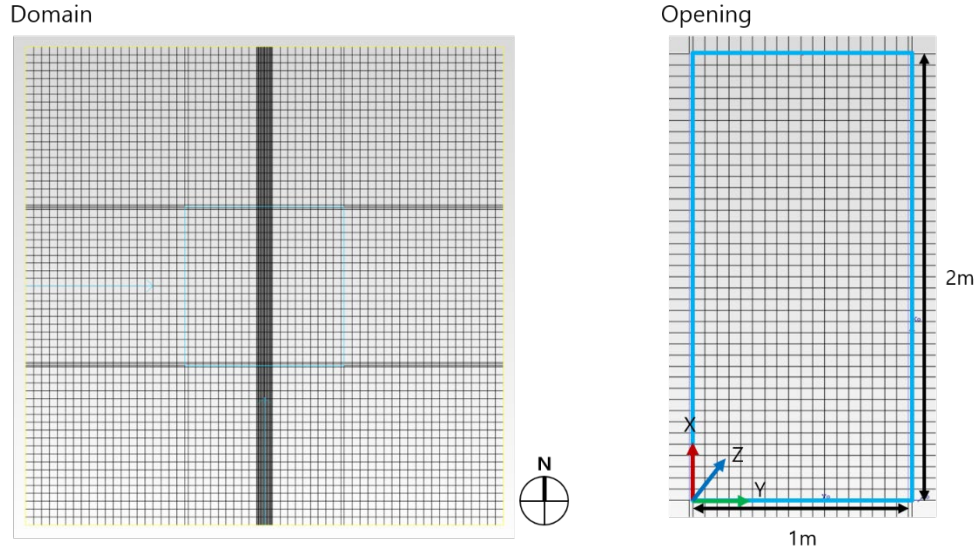
Figure 11: CFD simulation grid setting

Airflow rate (m^3/s) is calculated based on the multiplication between XY plane area of the cells in the openings and Z velocity of the wind passing through the cells, as shown in the Eqn. (3).

$$Q = \sum_{i=1}^{800}(A * V_{Zi}) \tag{3}$$

Where A is the XY plane area of a cell and V_{Zi} is the Z velocity of the wind passing through a cell.

2.2.2 CFD simulation cases

Total three types of opening scenarios were tested as in Figure 12. First, single-sided ventilation with one opening case. Second, cross ventilation with two adjacent openings. Third, cross ventilation with two openings facing the opposite. Each case can be subdivided further by opening directions.
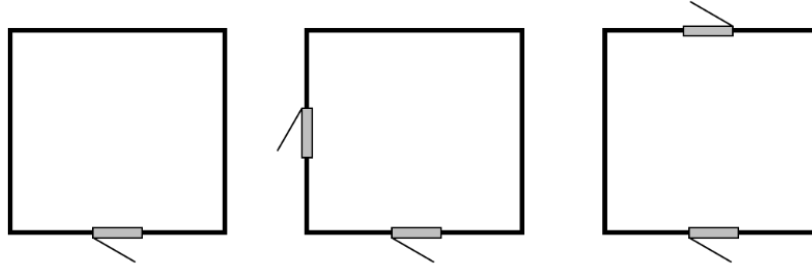
Figure 12: NV scenarios

Next, 36 wind directions ranging from 0° to 360° in increments of 10° were tested. This follows wind direction classification in the EnergyPlus weather file. In the case of the wind speeds, it was found from the test simulations that airflow is proportional to the wind speed. Figure 13 is the test simulations result showing the relationship of wind speed, louver opening angle, and airflow. Accordingly, only 1 m/s of wind case was tested as a benchmark.

Wind speed	Louver opening angle	
	30°	60°
0.5m/s	0.22	0.311
1m/s	0.42	0.617
1.5m/s	0.658	0.928
2m/s	0.87	1.232
2.5m/s	1.086	1.535
3m/s	1.298	1.834
3.5m/s	1.511	2.133
4m/s	1.723	2.444
4.5m/s	1.934	2.757
5m/s	2.143	3.062
5.5m/s	2.354	3.369
6m/s	2.563	3.677
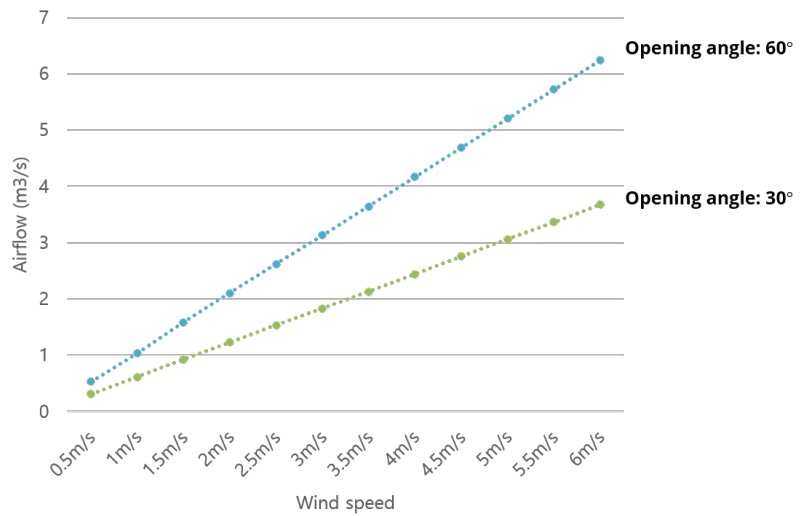
Figure 13: Wind speed, louver opening angle, and airflow relationship test result

Finally, louver opening angle ranging from 5° to 90° in increments of 5° were tested. Considering all the variables tested, Table 1 shows the number of airflow data created from the CFD simulations.

Table 1: Number of airflow data results created

	Wind directions (A)	Wind speed (B)	Opening directions (C)	Louver opening angles (D)	Control case (E)	Total cases A x B x C x (D+E)
Single-sided ventilation	36	1	4	18	1	2,592
Cross ventilation (adjacent openings)	36	1	4	18	1	2,592
Cross ventilation (opposite openings)	36	1	2	18	1	1,296

However, the actual number of CFD simulation runs was smaller than the number of airflow data created. As in Figure 14, symmetries on the models reduce wind directions and open directions to consider.
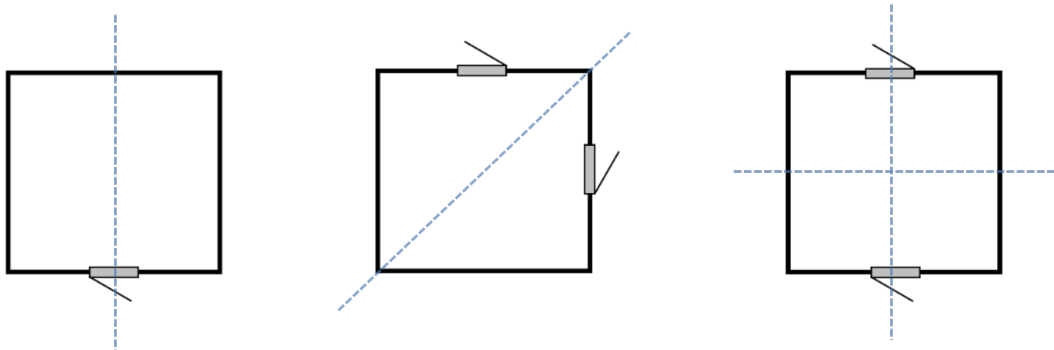
Figure 14: Symmetries on the models

Accordingly, the number of actual CFD simulation runs are shown in Table 2.

Table 2: Number of CFD simulation runs

	Wind directions (A)	Wind speed (B)	Opening directions (C)	Louver opening angles (D)	Control case (E)	Total runs A x B x C x (D+E)
Single-sided ventilation	18	1	1	18	1	324
Cross ventilation (adjacent openings)	18	1	1	18	1	324
Cross ventilation (opposite openings)	10	1	1	18	1	190

2.2.3 CFD simulation result

The visualizations in Figure 15 show a single-sided ventilation case with the south-facing opening that wind is blowing at $1m/s$ from 270° direction. Comparing the control case on the left and the experimental case with the louvers opened at 45° graphically shows a significant difference in airflow entering the space.
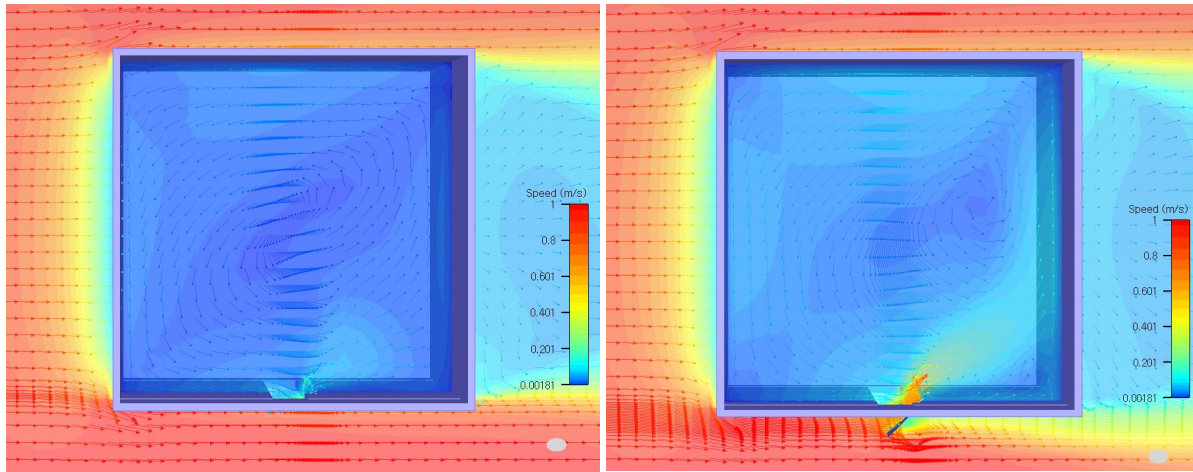
Figure 15: single-sided ventilation case sample result visualization (control case-left, cross experimental case-right)

The visualizations in Figure 16 show a cross ventilation case with the south-facing and north facing opening that wind is blowing at $1m/s$ from 270° direction. Comparing the control case on the left and the experimental case with the louvers opened at 45° graphically shows a significant difference in airflow entering the space.
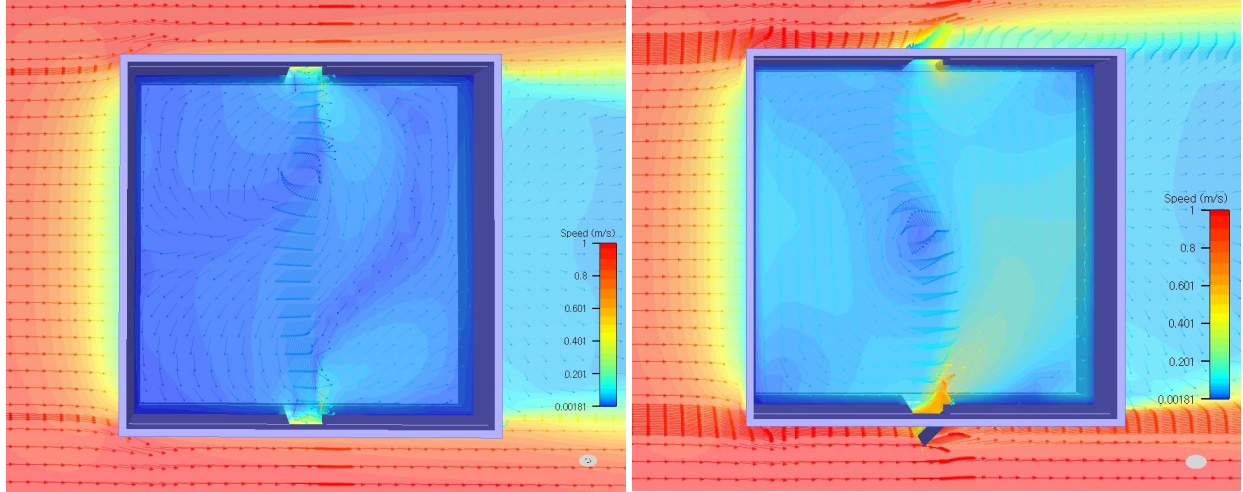
Figure 16: cross ventilation case sample result visualization (control case-left, cross experimental case-right)

Entire airflow results from CFD simulations are presented in the following pages. Table 3 is the airflow result of single-sided ventilation with south facing opening. Table 4 is the airflow result of cross ventilation with south and west facing opening. Table 5 is the airflow result of cross ventilation with south and north facing opening. By re-organizing the rows of the tables, cases for different opening directions can be found.

Table 3: Airflow result of single-sided ventilation with south facing opening

Wind direction (°)	Wind speed (m/s)	Experimental case (Louver opening angle)																			Control case
		5°	10°	15°	20°	25°	30°	35°	40°	45°	50°	55°	60°	65°	70°	75°	80°	85°	90°	180°	
0		0.001	0.001	0.001	0.001	0.001	0.001	0.002	0.002	0.002	0.002	0.002	0.002	0.002	0.002	0.003	0.003	0.002	0.002	0.002	0.002
10		0.003	0.004	0.005	0.005	0.006	0.007	0.007	0.007	0.007	0.007	0.007	0.007	0.008	0.007	0.006	0.006	0.005	0.005	0.005	0.005
20		0.003	0.005	0.005	0.007	0.007	0.009	0.01	0.011	0.011	0.011	0.012	0.011	0.01	0.009	0.009	0.009	0.008	0.007	0.006	0.006
30		0.004	0.006	0.007	0.008	0.009	0.011	0.011	0.015	0.015	0.015	0.015	0.015	0.015	0.013	0.012	0.012	0.012	0.01	0.009	0.009
40		0.005	0.008	0.008	0.011	0.014	0.014	0.014	0.018	0.018	0.018	0.019	0.02	0.021	0.018	0.017	0.015	0.016	0.012	0.01	0.01
50		0.005	0.007	0.009	0.012	0.014	0.014	0.018	0.022	0.023	0.024	0.025	0.021	0.018	0.021	0.021	0.022	0.016	0.015	0.011	0.011
60		0.006	0.008	0.016	0.018	0.018	0.014	0.019	0.021	0.021	0.02	0.019	0.018	0.018	0.017	0.016	0.016	0.016	0.015	0.014	0.014
70		0.004	0.005	0.006	0.006	0.008	0.012	0.019	0.022	0.031	0.031	0.035	0.035	0.035	0.036	0.034	0.036	0.037	0.038	0.017	0.017
80		0.027	0.048	0.064	0.077	0.095	0.116	0.138	0.152	0.166	0.169	0.17	0.176	0.174	0.176	0.173	0.171	0.168	0.169	0.015	0.015
90		0.055	0.09	0.125	0.151	0.176	0.195	0.211	0.226	0.231	0.231	0.227	0.226	0.218	0.214	0.208	0.209	0.212	0.216	0.023	0.023
100		0.063	0.102	0.141	0.169	0.2	0.225	0.244	0.266	0.279	0.278	0.274	0.276	0.27	0.266	0.259	0.252	0.25	0.25	0.032	0.032
110		0.073	0.111	0.152	0.183	0.215	0.239	0.259	0.276	0.285	0.284	0.276	0.275	0.269	0.267	0.261	0.256	0.254	0.256	0.033	0.033
120		0.075	0.116	0.16	0.192	0.225	0.248	0.265	0.278	0.287	0.282	0.276	0.274	0.269	0.266	0.263	0.257	0.254	0.254	0.034	0.034
130		0.069	0.111	0.153	0.186	0.218	0.242	0.259	0.273	0.282	0.275	0.269	0.27	0.265	0.263	0.262	0.259	0.255	0.254	0.05	0.05
140		0.058	0.1	0.139	0.168	0.2	0.223	0.242	0.256	0.265	0.26	0.255	0.255	0.248	0.244	0.241	0.238	0.237	0.239	0.076	0.076
150		0.054	0.085	0.12	0.146	0.175	0.198	0.216	0.229	0.238	0.232	0.226	0.223	0.218	0.212	0.207	0.205	0.205	0.208	0.066	0.066
160		0.042	0.07	0.097	0.12	0.144	0.167	0.185	0.198	0.206	0.201	0.194	0.185	0.178	0.171	0.165	0.162	0.16	0.164	0.068	0.068
170	1	0.033	0.051	0.07	0.088	0.106	0.125	0.144	0.169	0.169	0.167	0.166	0.163	0.155	0.149	0.14	0.131	0.123	0.123	0.09	0.09
180		0.014	0.025	0.033	0.044	0.05	0.06	0.072	0.08	0.092	0.102	0.112	0.117	0.121	0.126	0.131	0.132	0.132	0.134	0.09	0.09
190		0.033	0.051	0.07	0.088	0.106	0.125	0.144	0.169	0.169	0.167	0.166	0.163	0.155	0.149	0.14	0.131	0.123	0.123	0.09	0.09
200		0.042	0.07	0.097	0.12	0.144	0.167	0.185	0.198	0.206	0.201	0.194	0.185	0.178	0.171	0.165	0.162	0.16	0.164	0.068	0.068
210		0.054	0.085	0.12	0.146	0.175	0.198	0.216	0.229	0.238	0.232	0.226	0.223	0.218	0.212	0.207	0.205	0.205	0.208	0.066	0.066
220		0.058	0.1	0.139	0.168	0.2	0.223	0.242	0.256	0.265	0.26	0.255	0.255	0.248	0.244	0.241	0.238	0.237	0.239	0.076	0.076
230		0.069	0.111	0.153	0.186	0.218	0.242	0.259	0.273	0.282	0.275	0.269	0.27	0.265	0.263	0.262	0.259	0.255	0.254	0.05	0.05
240		0.075	0.116	0.16	0.192	0.225	0.248	0.265	0.278	0.287	0.282	0.276	0.274	0.269	0.266	0.263	0.257	0.254	0.254	0.034	0.034
250		0.073	0.111	0.152	0.183	0.215	0.239	0.259	0.276	0.285	0.284	0.276	0.275	0.269	0.267	0.261	0.256	0.254	0.256	0.033	0.033
260		0.063	0.102	0.141	0.169	0.2	0.225	0.244	0.266	0.279	0.278	0.274	0.276	0.27	0.266	0.259	0.252	0.25	0.25	0.032	0.032
270		0.055	0.09	0.125	0.151	0.176	0.195	0.211	0.226	0.231	0.231	0.227	0.226	0.218	0.214	0.208	0.209	0.212	0.216	0.023	0.023
280		0.027	0.048	0.064	0.077	0.095	0.116	0.138	0.152	0.166	0.169	0.17	0.176	0.174	0.176	0.173	0.171	0.168	0.169	0.015	0.015
290		0.004	0.005	0.006	0.006	0.008	0.012	0.019	0.022	0.031	0.031	0.035	0.035	0.035	0.036	0.034	0.036	0.037	0.038	0.017	0.017
300		0.006	0.008	0.016	0.018	0.018	0.014	0.019	0.021	0.021	0.02	0.019	0.018	0.018	0.017	0.016	0.016	0.016	0.015	0.014	0.014
310		0.005	0.007	0.009	0.012	0.014	0.014	0.018	0.022	0.023	0.024	0.025	0.021	0.018	0.021	0.021	0.022	0.016	0.015	0.011	0.011
320		0.005	0.008	0.008	0.011	0.014	0.014	0.014	0.018	0.018	0.018	0.019	0.02	0.021	0.018	0.017	0.015	0.016	0.012	0.01	0.01
330		0.004	0.006	0.007	0.008	0.009	0.011	0.011	0.015	0.015	0.015	0.015	0.015	0.015	0.013	0.012	0.012	0.012	0.01	0.009	0.009
340		0.003	0.005	0.005	0.007	0.007	0.009	0.01	0.011	0.011	0.011	0.012	0.011	0.01	0.009	0.009	0.009	0.008	0.007	0.006	0.006
350		0.003	0.004	0.005	0.005	0.006	0.007	0.007	0.007	0.007	0.007	0.007	0.007	0.008	0.007	0.006	0.006	0.005	0.005	0.005	0.005

Table 4: Airflow result of cross ventilation with south and west facing opening

Wind direction (°)	Wind speed (m/s)	Experimental case (Louver opening angle)																			Control case
		5°	10°	15°	20°	25°	30°	35°	40°	45°	50°	55°	60°	65°	70°	75°	80°	85°	90°	180°	
0		0.108	0.13	0.208	0.331	0.389	0.439	0.394	0.429	0.476	0.518	0.554	0.626	0.67	0.674	0.675	0.705	0.706	0.674	0.035	0.035
10		0.049	0.08	0.05	0.116	0.178	0.236	0.184	0.215	0.257	0.302	0.319	0.365	0.391	0.39	0.382	0.392	0.374	0.394	0.051	0.051
20		0.013	0.018	0.018	0.048	0.05	0.041	0.076	0.076	0.072	0.058	0.059	0.063	0.062	0.061	0.059	0.07	0.063	0.132	0.068	0.068
30		0.006	0.012	0.022	0.022	0.042	0.049	0.063	0.08	0.081	0.073	0.079	0.085	0.089	0.088	0.09	0.082	0.08	0.075	0.062	0.062
40		0.003	0.012	0.031	0.043	0.049	0.049	0.066	0.065	0.068	0.07	0.073	0.072	0.075	0.078	0.08	0.08	0.081	0.082	0.034	0.034
50		0.003	0.012	0.031	0.043	0.049	0.049	0.066	0.065	0.068	0.07	0.073	0.072	0.075	0.078	0.08	0.08	0.081	0.082	0.034	0.034
60		0.006	0.012	0.022	0.022	0.042	0.049	0.063	0.08	0.081	0.073	0.079	0.085	0.089	0.088	0.09	0.082	0.08	0.075	0.062	0.062
70		0.013	0.018	0.018	0.048	0.05	0.041	0.076	0.076	0.072	0.058	0.059	0.063	0.062	0.061	0.059	0.07	0.063	0.132	0.068	0.068
80		0.049	0.08	0.05	0.116	0.178	0.236	0.184	0.215	0.257	0.302	0.319	0.365	0.391	0.39	0.382	0.392	0.374	0.394	0.051	0.051
90		0.108	0.13	0.208	0.331	0.389	0.439	0.394	0.429	0.476	0.518	0.554	0.626	0.67	0.674	0.675	0.705	0.706	0.674	0.035	0.035
100		0.154	0.193	0.284	0.358	0.454	0.518	0.489	0.551	0.58	0.634	0.675	0.744	0.775	0.793	0.789	0.819	0.815	0.78	0.087	0.087
110		0.184	0.221	0.321	0.397	0.496	0.556	0.537	0.597	0.626	0.687	0.736	0.801	0.836	0.873	0.857	0.887	0.885	0.846	0.266	0.266
120		0.192	0.278	0.349	0.434	0.539	0.606	0.549	0.593	0.632	0.699	0.744	0.861	0.885	0.92	0.906	0.946	0.948	0.93	0.449	0.449
130		0.189	0.24	0.352	0.436	0.509	0.594	0.548	0.618	0.663	0.718	0.781	0.909	0.944	0.956	0.963	1.001	1.002	1.01	0.661	0.661
140		0.201	0.25	0.361	0.407	0.531	0.605	0.582	0.649	0.697	0.77	0.827	0.947	1.015	1.049	1.057	1.11	1.114	1.131	0.867	0.867
150		0.208	0.251	0.333	0.414	0.514	0.605	0.574	0.664	0.704	0.787	0.842	1.026	1.059	1.127	1.136	1.162	1.213	1.226	1.076	1.076
160		0.22	0.222	0.32	0.431	0.507	0.617	0.601	0.647	0.731	0.794	0.892	1.039	1.087	1.147	1.197	1.243	1.272	1.299	1.237	1.237
170	1	0.228	0.238	0.319	0.419	0.542	0.633	0.621	0.71	0.802	0.88	0.969	1.15	1.184	1.248	1.283	1.299	1.355	1.363	1.268	1.268
180		0.236	0.225	0.339	0.468	0.544	0.63	0.655	0.739	0.805	0.898	0.958	1.088	1.15	1.197	1.229	1.26	1.298	1.308	1.15	1.15
190		0.226	0.254	0.349	0.458	0.573	0.688	0.655	0.757	0.821	0.892	0.97	1.125	1.136	1.188	1.22	1.256	1.281	1.312	1.081	1.081
200		0.188	0.244	0.357	0.428	0.551	0.648	0.617	0.719	0.801	0.897	0.987	1.094	1.12	1.164	1.196	1.218	1.233	1.261	0.915	0.915
210		0.169	0.242	0.347	0.427	0.536	0.614	0.585	0.681	0.744	0.824	0.91	1.048	1.068	1.114	1.131	1.183	1.19	1.206	0.438	0.438
220		0.149	0.226	0.324	0.395	0.511	0.607	0.556	0.622	0.688	0.746	0.809	0.921	0.97	1.006	1.022	1.052	1.062	1.08	0.277	0.277
230		0.149	0.226	0.324	0.395	0.511	0.607	0.556	0.622	0.688	0.746	0.809	0.921	0.97	1.006	1.022	1.052	1.062	1.08	0.277	0.277
240		0.169	0.242	0.347	0.427	0.536	0.614	0.585	0.681	0.744	0.824	0.91	1.048	1.068	1.114	1.131	1.183	1.19	1.206	0.438	0.438
250		0.188	0.244	0.357	0.428	0.551	0.648	0.617	0.719	0.801	0.897	0.987	1.094	1.12	1.164	1.196	1.218	1.233	1.261	0.915	0.915
260		0.226	0.254	0.349	0.458	0.573	0.688	0.655	0.757	0.821	0.892	0.97	1.125	1.136	1.188	1.22	1.256	1.281	1.312	1.081	1.081
270		0.236	0.225	0.339	0.468	0.544	0.63	0.655	0.739	0.805	0.898	0.958	1.088	1.15	1.197	1.229	1.26	1.298	1.308	1.15	1.15
280		0.228	0.238	0.319	0.419	0.542	0.633	0.621	0.71	0.802	0.88	0.969	1.15	1.184	1.248	1.283	1.299	1.355	1.363	1.268	1.268
290		0.22	0.222	0.32	0.431	0.507	0.617	0.601	0.647	0.731	0.794	0.892	1.039	1.087	1.147	1.197	1.243	1.272	1.299	1.237	1.237
300		0.208	0.251	0.333	0.414	0.514	0.605	0.574	0.664	0.704	0.787	0.842	1.026	1.059	1.127	1.136	1.162	1.213	1.226	1.076	1.076
310		0.201	0.25	0.361	0.407	0.531	0.605	0.582	0.649	0.697	0.77	0.827	0.947	1.015	1.049	1.057	1.11	1.114	1.131	0.867	0.867
320		0.189	0.24	0.352	0.436	0.509	0.594	0.548	0.618	0.663	0.718	0.781	0.909	0.944	0.956	0.963	1.001	1.002	1.01	0.661	0.661
330		0.192	0.278	0.349	0.434	0.539	0.606	0.549	0.593	0.632	0.699	0.744	0.861	0.885	0.92	0.906	0.946	0.948	0.93	0.449	0.449
340		0.184	0.221	0.321	0.397	0.496	0.556	0.537	0.597	0.626	0.687	0.736	0.801	0.836	0.873	0.857	0.887	0.885	0.846	0.266	0.266
350		0.154	0.193	0.284	0.358	0.454	0.518	0.489	0.551	0.58	0.634	0.675	0.744	0.775	0.793	0.789	0.819	0.815	0.78	0.087	0.087

24

Table 5: Airflow result of cross ventilation with north and south facing opening

Wind direction (°)	Wind speed (m/s)	Experimental case (Louver opening angle)																			Control case
		5°	10°	15°	20°	25°	30°	35°	40°	45°	50°	55°	60°	65°	70°	75°	80°	85°	90°	180°	
0		0.13	0.165	0.285	0.394	0.481	0.542	0.675	0.728	0.789	0.869	0.956	1.007	1.062	1.149	1.244	1.275	1.281	1.349	1.512	1.512
10		0.135	0.174	0.283	0.369	0.501	0.581	0.677	0.769	0.826	0.921	0.994	1.063	1.119	1.162	1.222	1.263	1.296	1.327	1.331	1.331
20		0.115	0.167	0.279	0.353	0.494	0.578	0.66	0.742	0.793	0.887	0.961	1.023	1.08	1.129	1.167	1.215	1.256	1.297	1.28	1.28
30		0.107	0.17	0.282	0.352	0.489	0.572	0.635	0.711	0.773	0.843	0.886	0.952	1.007	1.058	1.103	1.113	1.171	1.18	1.08	1.08
40		0.159	0.178	0.289	0.35	0.5	0.582	0.599	0.675	0.706	0.745	0.787	0.835	0.865	0.904	0.921	0.945	0.98	0.999	0.868	0.868
50		0.115	0.208	0.318	0.368	0.501	0.557	0.565	0.642	0.691	0.753	0.778	0.813	0.879	0.915	0.928	0.935	0.951	1.003	0.642	0.642
60		0.108	0.197	0.31	0.358	0.501	0.541	0.562	0.624	0.66	0.711	0.741	0.795	0.805	0.848	0.872	0.876	0.872	0.874	0.245	0.245
70		0.13	0.206	0.305	0.344	0.473	0.519	0.533	0.59	0.624	0.66	0.697	0.724	0.748	0.764	0.768	0.782	0.8	0.785	0.209	0.209
80		0.051	0.138	0.245	0.302	0.425	0.472	0.535	0.57	0.601	0.653	0.672	0.702	0.715	0.753	0.749	0.746	0.757	0.769	0.035	0.035
90		0.071	0.137	0.194	0.258	0.384	0.42	0.422	0.469	0.49	0.53	0.582	0.617	0.61	0.63	0.648	0.671	0.679	0.677	0.003	0.003
100		0.051	0.138	0.245	0.302	0.425	0.472	0.535	0.57	0.601	0.653	0.672	0.702	0.715	0.753	0.749	0.746	0.757	0.769	0.035	0.035
110		0.13	0.206	0.305	0.344	0.473	0.519	0.533	0.59	0.624	0.66	0.697	0.724	0.748	0.764	0.768	0.782	0.8	0.785	0.209	0.209
120		0.108	0.197	0.31	0.358	0.501	0.541	0.562	0.624	0.66	0.711	0.741	0.795	0.805	0.848	0.872	0.876	0.872	0.874	0.245	0.245
130		0.115	0.208	0.318	0.368	0.501	0.557	0.565	0.642	0.691	0.753	0.778	0.813	0.879	0.915	0.928	0.935	0.951	1.003	0.642	0.642
140		0.159	0.178	0.289	0.35	0.5	0.582	0.599	0.675	0.706	0.745	0.787	0.835	0.865	0.904	0.921	0.945	0.98	0.999	0.868	0.868
150		0.107	0.17	0.282	0.352	0.489	0.572	0.635	0.711	0.773	0.843	0.886	0.952	1.007	1.058	1.103	1.113	1.171	1.18	1.08	1.08
160		0.115	0.167	0.279	0.353	0.494	0.578	0.66	0.742	0.793	0.887	0.961	1.023	1.08	1.129	1.167	1.215	1.256	1.297	1.28	1.28
170	1	0.135	0.174	0.283	0.369	0.501	0.581	0.677	0.769	0.826	0.921	0.994	1.063	1.119	1.162	1.222	1.263	1.296	1.327	1.331	1.331
180		0.13	0.165	0.285	0.394	0.481	0.542	0.675	0.728	0.789	0.869	0.956	1.007	1.062	1.149	1.244	1.275	1.281	1.349	1.512	1.512
190		0.135	0.174	0.283	0.369	0.501	0.581	0.677	0.769	0.826	0.921	0.994	1.063	1.119	1.162	1.222	1.263	1.296	1.327	1.331	1.331
200		0.115	0.167	0.279	0.353	0.494	0.578	0.66	0.742	0.793	0.887	0.961	1.023	1.08	1.129	1.167	1.215	1.256	1.297	1.28	1.28
210		0.107	0.17	0.282	0.352	0.489	0.572	0.635	0.711	0.773	0.843	0.886	0.952	1.007	1.058	1.103	1.113	1.171	1.18	1.08	1.08
220		0.159	0.178	0.289	0.35	0.5	0.582	0.599	0.675	0.706	0.745	0.787	0.835	0.865	0.904	0.921	0.945	0.98	0.999	0.868	0.868
230		0.115	0.208	0.318	0.368	0.501	0.557	0.565	0.642	0.691	0.753	0.778	0.813	0.879	0.915	0.928	0.935	0.951	1.003	0.642	0.642
240		0.108	0.197	0.31	0.358	0.501	0.541	0.562	0.624	0.66	0.711	0.741	0.795	0.805	0.848	0.872	0.876	0.872	0.874	0.245	0.245
250		0.13	0.206	0.305	0.344	0.473	0.519	0.533	0.59	0.624	0.66	0.697	0.724	0.748	0.764	0.768	0.782	0.8	0.785	0.209	0.209
260		0.051	0.138	0.245	0.302	0.425	0.472	0.535	0.57	0.601	0.653	0.672	0.702	0.715	0.753	0.749	0.746	0.757	0.769	0.035	0.035
270		0.071	0.137	0.194	0.258	0.384	0.42	0.422	0.469	0.49	0.53	0.582	0.617	0.61	0.63	0.648	0.671	0.679	0.677	0.003	0.003
280		0.051	0.138	0.245	0.302	0.425	0.472	0.535	0.57	0.601	0.653	0.672	0.702	0.715	0.753	0.749	0.746	0.757	0.769	0.035	0.035
290		0.13	0.206	0.305	0.344	0.473	0.519	0.533	0.59	0.624	0.66	0.697	0.724	0.748	0.764	0.768	0.782	0.8	0.785	0.209	0.209
300		0.108	0.197	0.31	0.358	0.501	0.541	0.562	0.624	0.66	0.711	0.741	0.795	0.805	0.848	0.872	0.876	0.872	0.874	0.245	0.245
310		0.115	0.208	0.318	0.368	0.501	0.557	0.565	0.642	0.691	0.753	0.778	0.813	0.879	0.915	0.928	0.935	0.951	1.003	0.642	0.642
320		0.159	0.178	0.289	0.35	0.5	0.582	0.599	0.675	0.706	0.745	0.787	0.835	0.865	0.904	0.921	0.945	0.98	0.999	0.868	0.868
330		0.107	0.17	0.282	0.352	0.489	0.572	0.635	0.711	0.773	0.843	0.886	0.952	1.007	1.058	1.103	1.113	1.171	1.18	1.08	1.08
340		0.115	0.167	0.279	0.353	0.494	0.578	0.66	0.742	0.793	0.887	0.961	1.023	1.08	1.129	1.167	1.215	1.256	1.297	1.28	1.28
350		0.135	0.174	0.283	0.369	0.501	0.581	0.677	0.769	0.826	0.921	0.994	1.063	1.119	1.162	1.222	1.263	1.296	1.327	1.331	1.331

Results were visualized into charts to better understand the effect of the louvers. The case without the louvers is colored in red, and the case with the louvers is colored in blue.

Figure 17 shows Result visualization of single-sided ventilation with south facing opening. According to the figure, utilizing the louver brings higher airflow in entire directions. However, when the wind is blowing from the north, northeast, and northwest, airflow decreases significantly because the louvers do not receive sufficient pressure from wind flow.
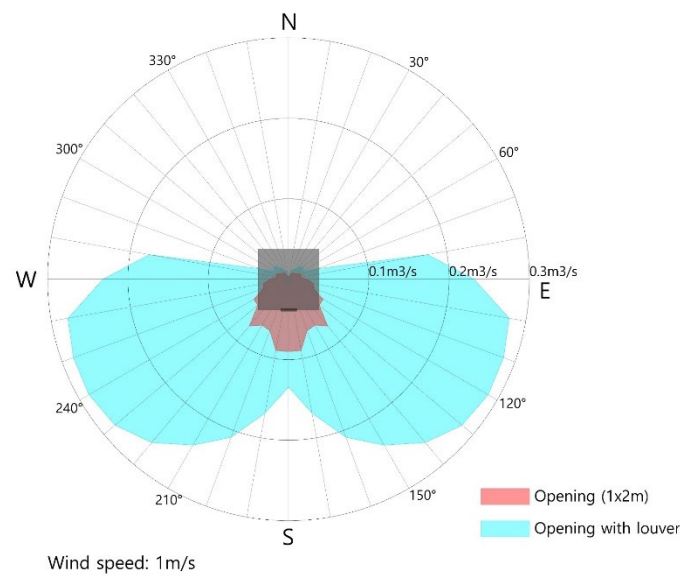
Figure 17: Result visualization of single-sided ventilation with south facing opening

Figure 18 shows Result visualization of cross ventilation with south and west facing opening. According to the figure, utilizing the louver brings higher airflow in entire directions. However, when the wind is blowing from the northeast, airflow decreases significantly because the louvers do not receive sufficient pressure from wind flow.
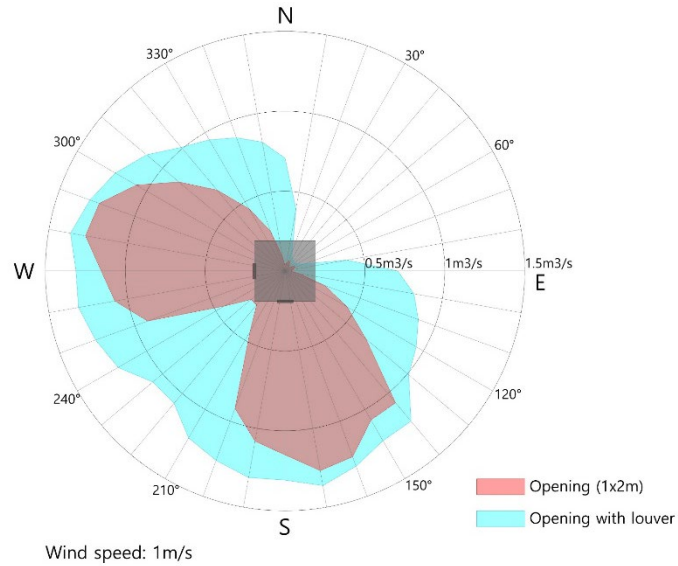
Figure 18: Result visualization of cross ventilation with south and west facing opening

Figure 19 shows Result visualization of cross ventilation with north and south facing opening. According to the figure, utilizing the louver brings equal or higher airflow in entire directions.
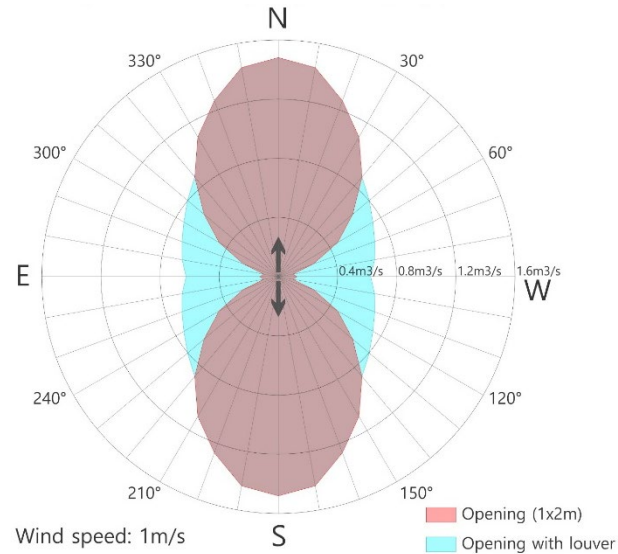
Figure 19: Result visualization of cross ventilation with north and south facing opening

In conclusion, the louver performance CFD simulation test that measured airflow passing through the openings has proved that the louvers can control the pressure between the openings

and result in higher airflow into space. Based on the data collected, whether the louvers can bring higher NV potential will be tested further in the following sections.

2.3 Control system design

The control system that can determine whether each hour is a spatial NV hour and outputs opening angle of the louvers was designed. The workflow chart is illustrated in Figure 20.
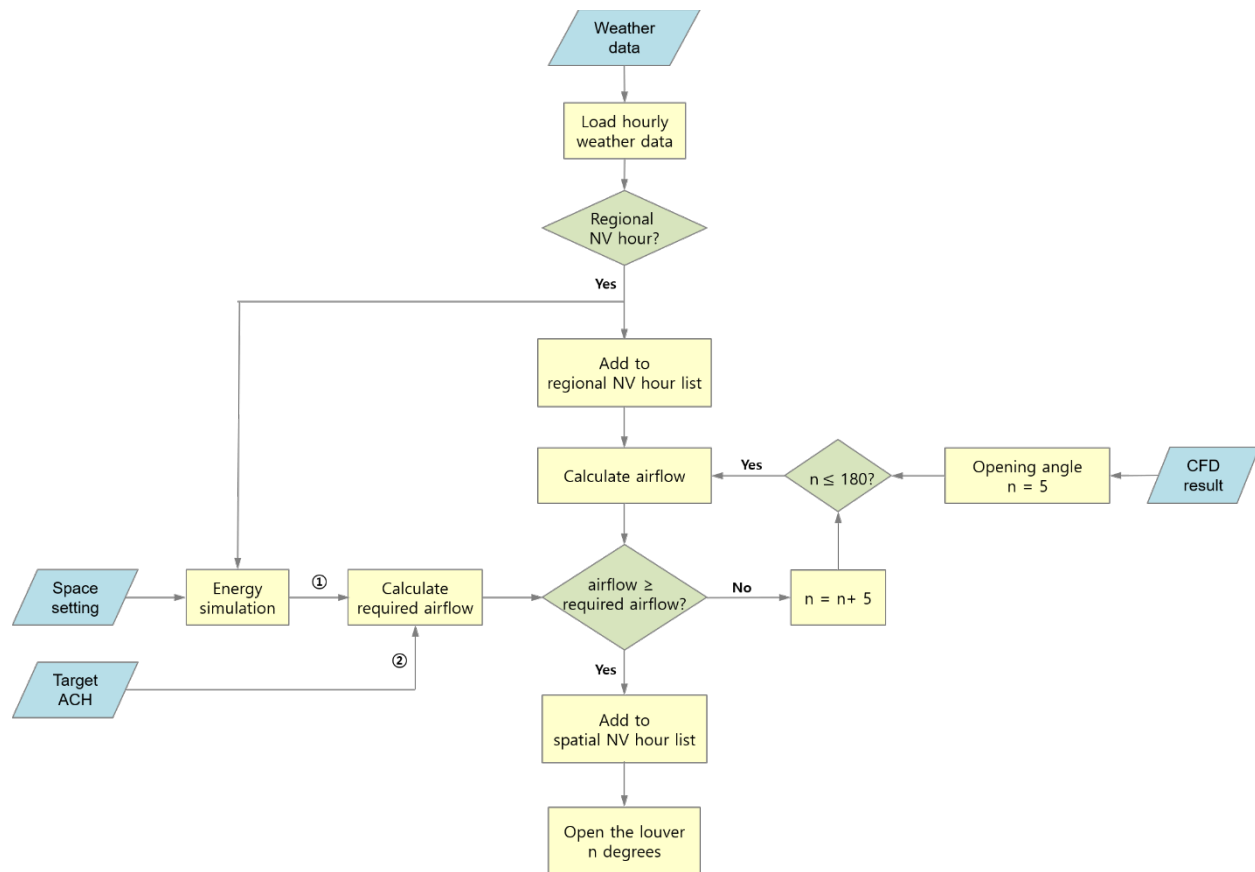
Figure 20: Louver control system workflow chart

The first step of the workflow is loading hourly weather data from the weather data. Then each hour is tested if it is regional NV hour. If a given hour is regional NV hour, it is added to the regional NV hour list. Then, following the space setting and target ACH defined, required

airflow is calculated. At the same time, based on the airflow result from the CFD simulation and the weather data, airflow is calculated by setting the initial opening angle to five degrees. If the airflow is smaller than the required airflow, five is added to the opening angle with an upper limit of 180 degrees, and airflow calculation is iterated. When airflow gets bigger or equal to the required airflow, that hour is added to the spatial NV hour list and commands the louver to open with the opening angle found. These steps are repeated for 8,760 hours in a typical year.

2.4 Simulation tool

A simulation tool was developed to understand better the data set results from CFD simulations and to embed control system proposed. The simulation tool outputs NV potential and cooling energy saving potential in various locations and building configurations, including regional scale, spatial scale without the louvers, and spatial scale with the louvers. By using the simulation tool, architects and engineers will be able to design naturally ventilation buildings with reliable results.

2.4.1 Platform

The simulation tool is built on existing Rhinoceros and Grasshopper modeling platforms. Rhinoceros is one of the most well-known and widely used platforms for 3D modeling tools for architects and engineers. Grasshopper is a graphical algorithm editor plugin for Rhinoceros. Plugins of Grasshopper are used to assist the workflow of simulation. Ladybug, a plugin for environmentally-informed design, is included to produce hourly weather data from the EnergyPlus weather file. Honeybee, an energy modeling plugin using OpenStudio as an engine, is used in the simulation to load DOE Prototype Building and DOE Reference Building models,

writing the IDF files and running the energy simulation. Lastly, Python scripts were coded on the Grasshopper canvas for calculations and processing data.
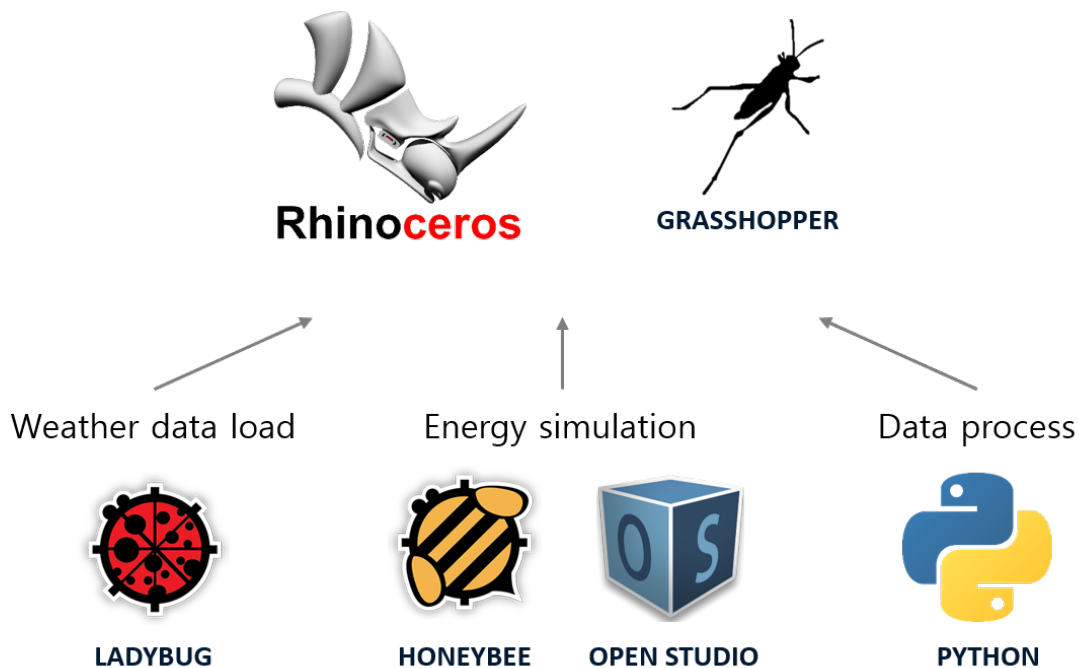
Figure 21: The simulation tool configuration

2.4.2 Features of the tool

The simulation tool is mainly divided into three parts, as shown in Figure 22. The Setting part allows users to set building location, building program, etc. The Simulation & data process part receives data and performs calculations to determine NV potential. The Visualization part receives results and visualize them in Rhinoceros.
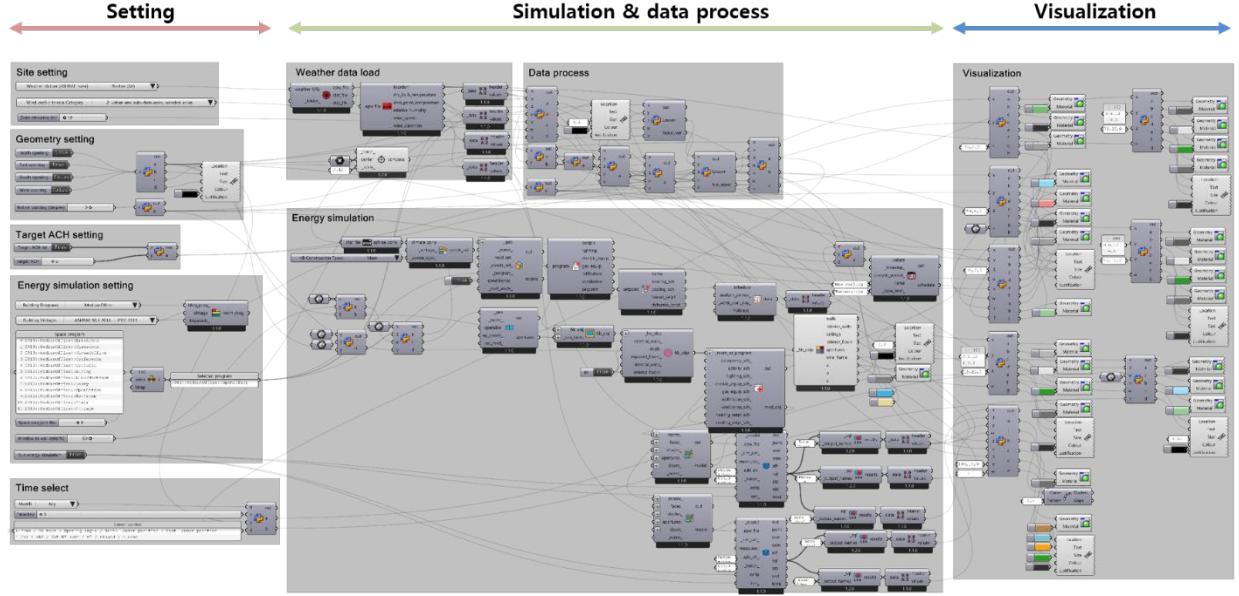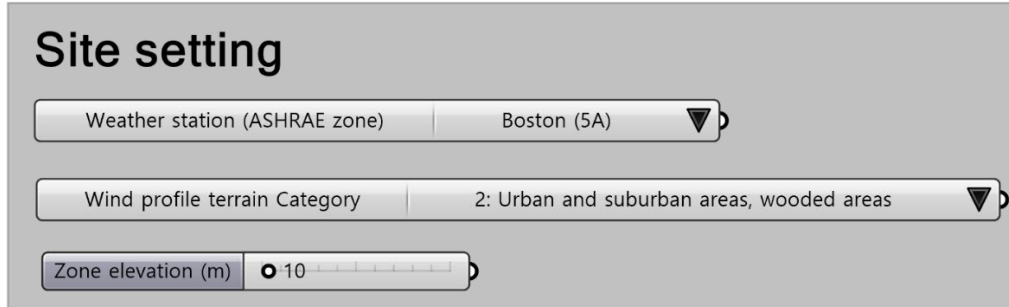
Figure 22: The simulation tool Grasshopper script overview

The Site setting shown in Figure 23 is comprised of three components. The user can select one of the weather stations provided in the simulation tool or manually load the EnergyPlus weather file they possess. Next, users can select one of Wind profile terrain category according to site surrounding environment and set Zone elevation in meters. This setting is used to calibrate wind speed at the weather station to local wind speed (m/s) at the site following the Eqn. (4) provided in ASHRAE Fundamentals (2017).

$$U_H = U_{met} \left(\frac{\delta_{met}}{H_{met}}\right)^{\alpha_{met}} \left(\frac{H}{\delta}\right)^{\alpha} \tag{4}$$

Where U_{met} is a wind speed at the weather station, δ_{met} is atmospheric boundary layer thickness for the weather station, H_{met} is the height of the weather station, α_{met} is the exponent for the weather station. Similarly, H is the height to calculate local wind speed, δ is the atmospheric

boundary layer thickness for the local building terrain, and α is the exponent for the local

building terrain.

Figure 23: Site setting components in Grasshopper canvas

After the Site setting is done, the Regional NV hour chart and the NV hour wind frequency chart

are presented on the Rhinoceros viewport. The Regional NV hour chart, which shows hours

when natural ventilation is available at the region around the weather station according to the

Eqn. (1). The users can find month and date in the X-axis and find a specific hour of a day in the

Y-axis to determine if that hour is NV hour or Non-NV hour. The sample case of Boston in

Figure 24 shows a total of 2,745 hours out of the 8,760 hours in a typical year (31.3%) is

regional NV hours.
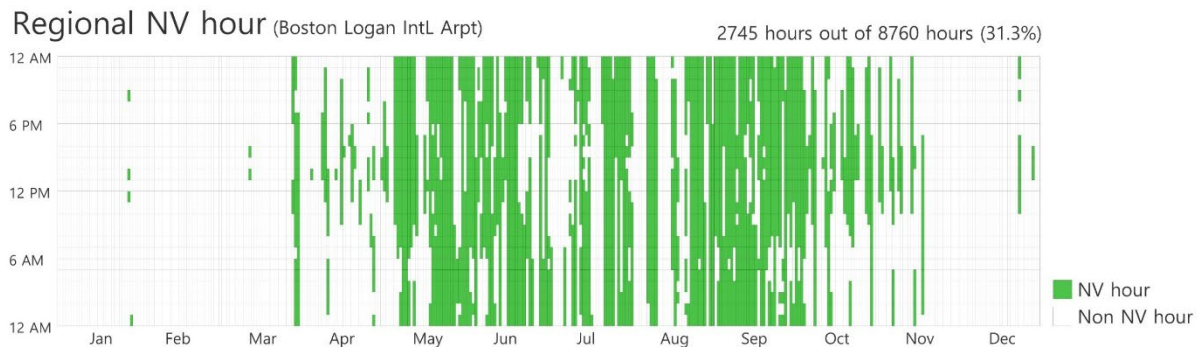
Figure 24: The Regional NV hour chart visualized in the Rhinoceros viewport

The NV hour wind frequency chart shows wind patterns during NV hours. Each thirty-six direction represent wind frequency in a percentage value. The sample case of Boston in Figure 25 shows a high percentage of northwest wind and southwest wind during the NV hours.
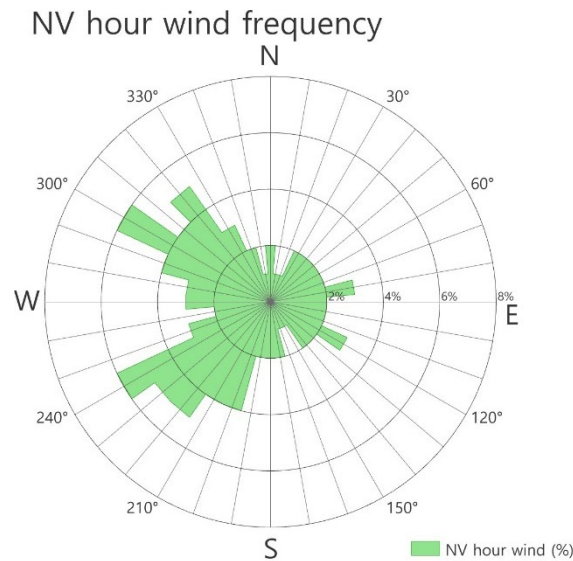
Figure 25: The NV hour wind frequency chart visualized in the Rhinoceros viewport

After the Site setting, the Geometry setting indicated in Figure 26 asks users to define the number of openings and their orientation. Users can select one or two out of four orientations given and rotate the building in degree values to adjust building orientation in detail.
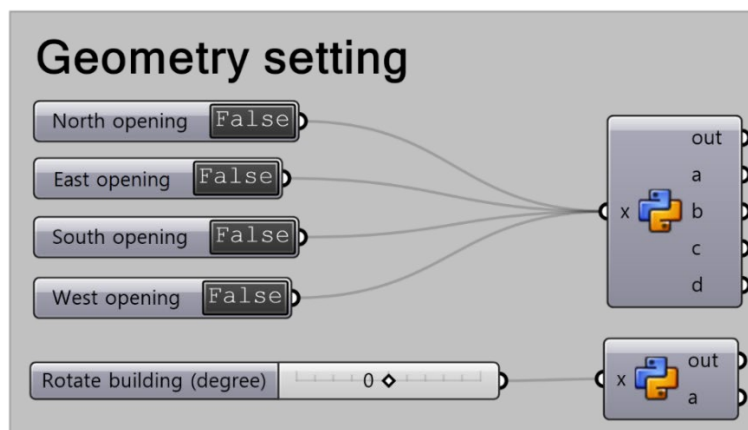
Figure 26: Geometry setting components in Grasshopper canvas

Change in the Geometry setting is synchronized as a visualization in the Rhinoceros viewport as in Figure 27.
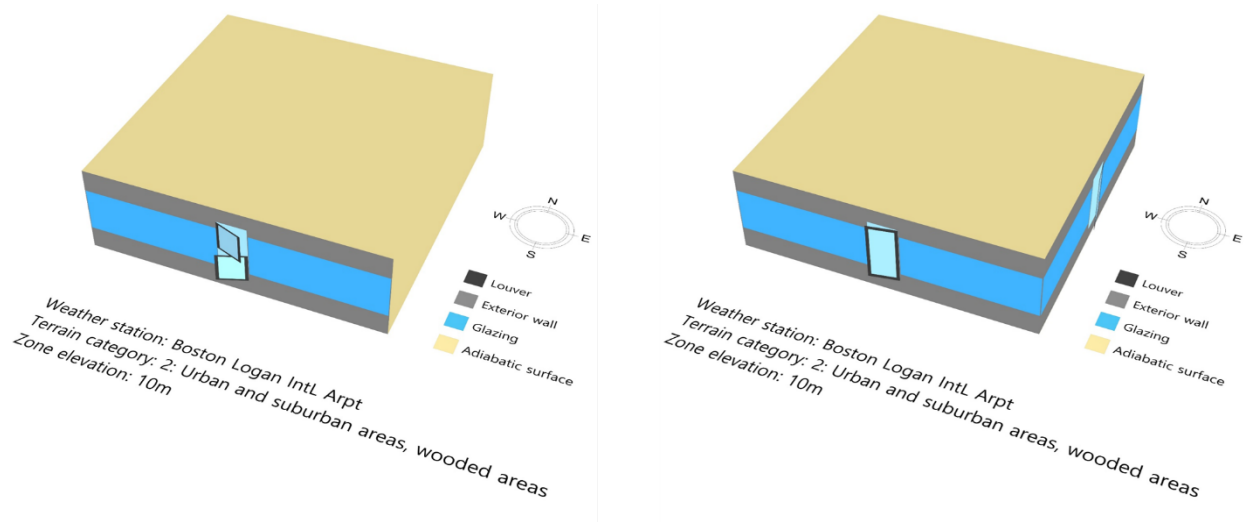
Figure 27: Geometry setting visualized in the Rhinoceros viewport (single-sided ventilation case-left, cross ventilation case-right)

Additionally, the NV mean airflow by direction chart is rendered in the Rhinoceros viewport as in Figure 28. This chart is a merge of the NV hour wind frequency chart and the NV potential chart.
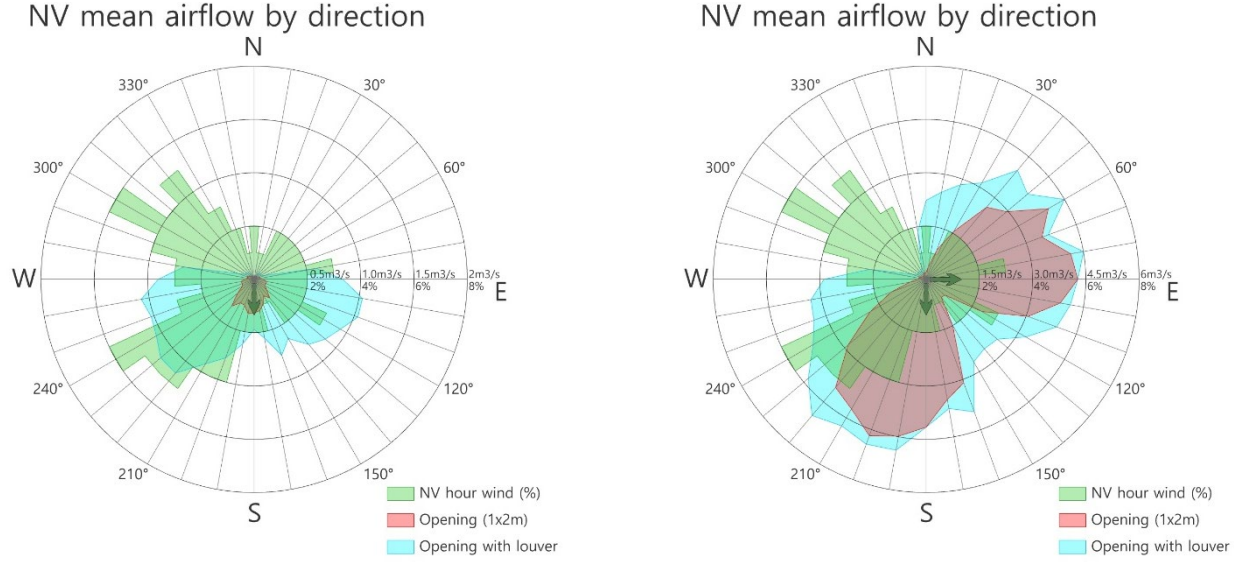
Figure 28: The NV mean airflow by direction chart visualized in the Rhinoceros viewport (single-sided ventilation case-left, cross ventilation case-right)

The red region shows the mean airflow of each direction in case of opening without the louver. The blue region shows the mean airflow of each direction in case of opening with the louver. The mean airflow rate (m^3/s) is calculated according to Eqn. (5).

$$\text{Mean airflow} = U_{average} * V_{max,1m/s} \tag{5}$$

Where $U_{average}$ is average wind speed (m/s) from a certain direction and $V_{max,1m/s}$ is maximum possible airflow rate (m^3/s) through the opening at 1m/s of wind from a certain direction.

The NV mean airflow by direction chart is presented to assist users in determining which directions to place openings. To receive maximum hours of wind and high airflow, users can choose opening directions and rotate the building.

Next, users can set target ACH at the Target ACH setting shown in Figure 29.
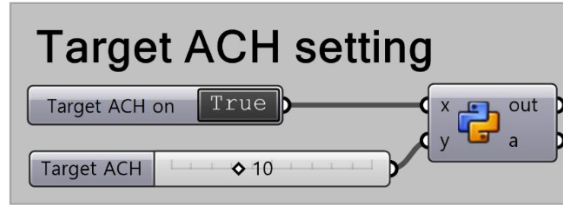
Figure 29: Target ACH setting components in Grasshopper canvas

By setting target ACH, hourly required airflow rate (m^3/h) is calculated according to Eqn. (6).

$$Q_{required} = ACH * V_{space} \qquad (6)$$

Where ACH is air changes per hour (n/h) and V_{space} is volume of the space (m^3).

Then hourly required airflow is compared with maximum possible airflow at corresponding hours. If a given hour is a regional NV hour and maximum possible airflow is equal or greater than the required airflow, that hour can be defined as spatial NV hour. Table 6 is an example of determining spatial NV hours by ACH setting.

Table 6: Example of determining spatial NV hour by ACH setting

Time	Regional NV hour	Target ACH	ACH required airflow	Maximum airflow	Spatial NV hour
22-Apr-17 4 PM	True	10	3,000	5,600	True
22-Apr-17 5 PM	True	10	3,000	2,600	False
22-Apr-17 6 PM	False	-	-	-	False
22-Apr-17 7 PM	False	-	-	-	False
22-Apr-17 8 PM	True	10	3,000	4,300	True
⋮	⋮	⋮	⋮	⋮	⋮
20-Nov-20 2 PM	False	-	-	-	False
20-Nov-20 3 PM	True	10	3,000	1,800	False
20-Nov-20 4 PM	True	10	3,000	4,500	True
20-Nov-20 5 PM	False	-	-	-	False
20-Nov-20 6 PM	True	10	3,000	4,800	True

Users can utilize energy simulation by controlling the Energy simulation setting presented in Figure 30. ACH setting and energy simulation can be used independently or at the same time. Twenty-three DOE Prototype Building and DOE Reference Building models are provided in the Building Programs component. Users can set the version of the model at the Building Vintages component and select specific space prom at the Space program component. Finally, window to wall ratio can be set in a percentage value at the Window to wall ratio component.
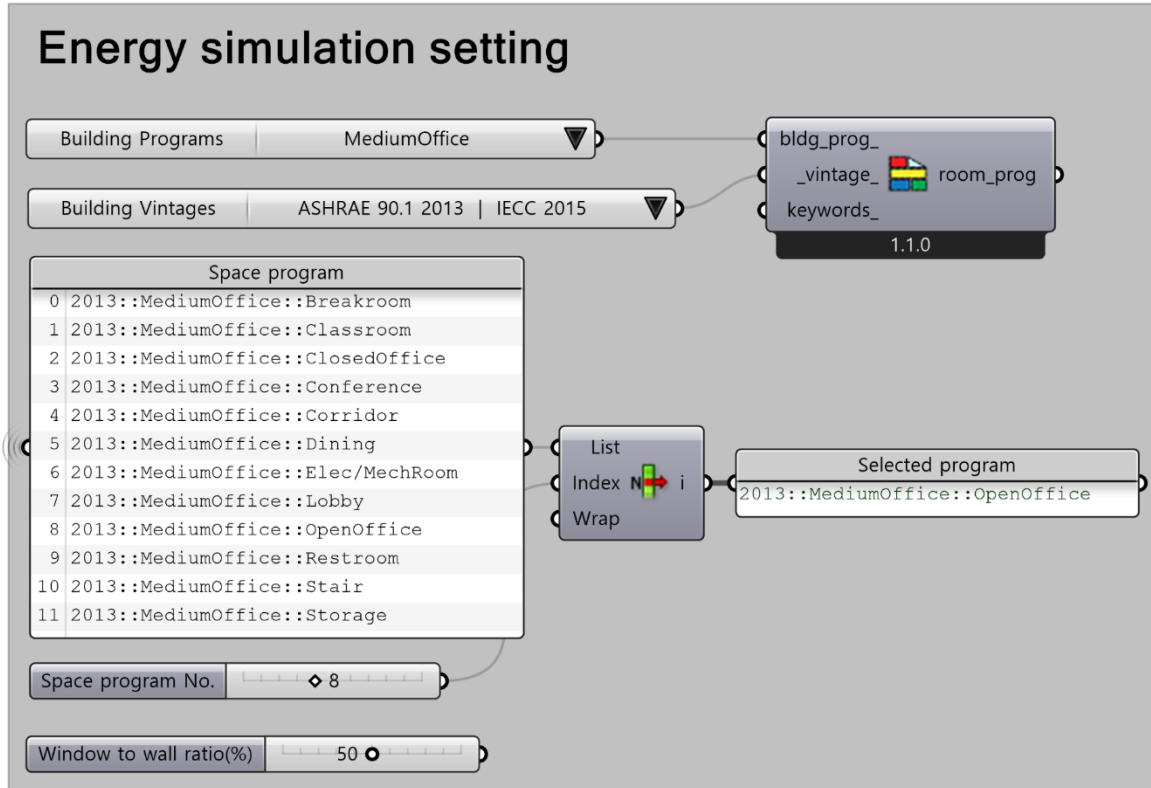
Figure 30: Energy simulation setting components in Grasshopper canvas

When energy simulation is done, hourly required airflow is calculated based on hourly sensible

cooling load and hourly CO_2 level. The hourly required airflow of the space to compensate for

the sensible cooling load (m^3/h) is calculated by the sensible heat equation defined by

ASHRAE Fundamentals (2017) as in Eqn. (7).

$$Q_{S-required} = \frac{q_s}{\rho * C_p * \Delta T} \tag{7}$$

Where q_s is amount of sensible cooling load, ρ is air density, C_p is specific heat of air, and ΔT is

a temperature difference between indoors setpoint and outdoors.

The hourly required airflow of the space to maintain the CO_2 level under the designated threshold (m^3/h) is calculated by the CO_2 concentration equation defined by ASHRAE Standard 62.1 (2016) as in Eqn. (8).

$$Q_{CO_2-required} = \frac{10^6 * S}{C_i - C_o} \qquad (8)$$

Where S is CO_2 strength, C_i is indoor CO_2 concentration set point, C_o is outdoor CO_2 concentration. The difference between C_i and C_o is set to 700ppm following the case in ASHRAE Standard 62.1 (2016).

After hourly required airflows for sensible cooling and CO_2 flushing are calculated, the one with a higher value is selected and compared with maximum possible airflow at corresponding hours. If a given hour is a regional NV hour and maximum possible airflow is equal or greater than the required airflow, that hour can be defined as spatial NV hour. Table 7 is an example of determining spatial NV hours by energy simulation.

Table 7: Example of determining spatial NV hour by energy simulation

Time	Regional NV hour	Energy simulation required airflow	Maximum airflow	Spatial NV hour
22-Apr-17 4 PM	True	4,800	5,600	True
22-Apr-17 5 PM	True	2,800	2,600	False
22-Apr-17 6 PM	False		-	False
22-Apr-17 7 PM	False		-	False
22-Apr-17 8 PM	True	2,500	4,300	True
⋮	⋮		⋮	⋮
20-Nov-20 2 PM	False		-	False
20-Nov-20 3 PM	True	4,300	1,800	False
20-Nov-20 4 PM	True	2,700	4,500	True
20-Nov-20 5 PM	False		-	False
20-Nov-20 6 PM	True	5,300	4,800	False

When target ACH and energy simulation are selected simultaneously, one of hourly required airflow with the higher value calculated is selected and compared with maximum possible airflow at corresponding hours. If a given hour is a regional NV hour and maximum possible airflow is equal or greater than the required airflow, that hour can be defined as spatial NV hour. Table 8 is an example of determining spatial NV hours by target ACH and energy simulation.

Table 8: Example of determining spatial NV hour by target ACH and energy simulation

Time	Regional NV hour	Target ACH	ACH required airflow	Energy simulation required airflow	Maximum airflow	Spatial NV hour
22-Apr-17 4 PM	True	10	3,000	4,800	5,600	True
22-Apr-17 5 PM	True	10	3,000	2,800	2,600	False
22-Apr-17 6 PM	False	-	-		-	False
22-Apr-17 7 PM	False	-	-		-	False
22-Apr-17 8 PM	True	10	3,000	2,500	4,300	True
⋮	⋮	⋮	⋮	⋮	⋮	⋮
20-Nov-20 2 PM	False	-	-		-	False
20-Nov-20 3 PM	True	10	3,000	4,300	1,800	False
20-Nov-20 4 PM	True	10	3,000	2,700	4,500	True
20-Nov-20 5 PM	False	-	-		-	False
20-Nov-20 6 PM	True	10	3,000	5,300	4,800	False

After spatial NV hours are defined, the Spatial NV hour charts appear in the Rhinoceros viewport. Spatial NV hour chart example in Figure 31 shows the annual spatial NV hours with a target ACH of 10 in an office building located at Boston without the louvers. Total 861 hours were deducted compared to regional NV hours due to insufficient airflow, and cells are marked in gray.
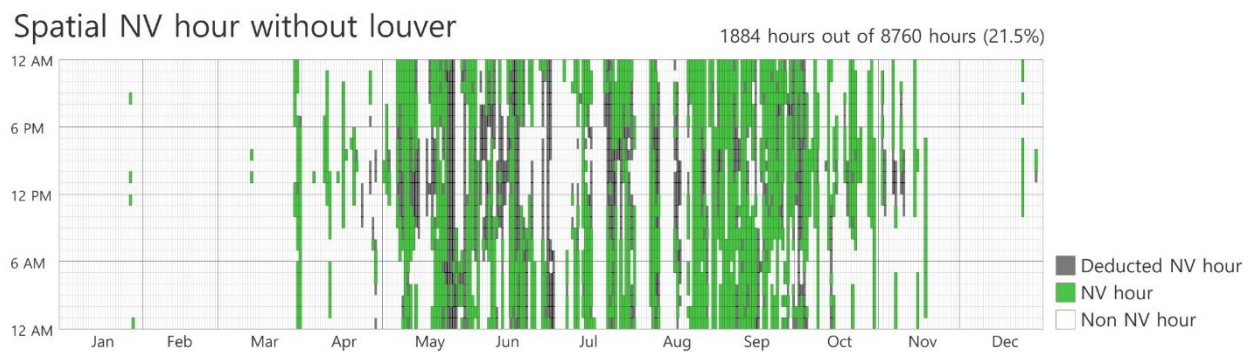
Figure 31: The Spatial NV hour chart without the use of louver visualized in the Rhinoceros viewport

Next, the Spatial NV hour chart example in Figure 32 shows the annual spatial NV hours with a target ACH of 10 in an office building located in Boston with the louvers. Total 403 hours were deducted compared to regional NV hours due to insufficient airflow, and cells are marked in gray.
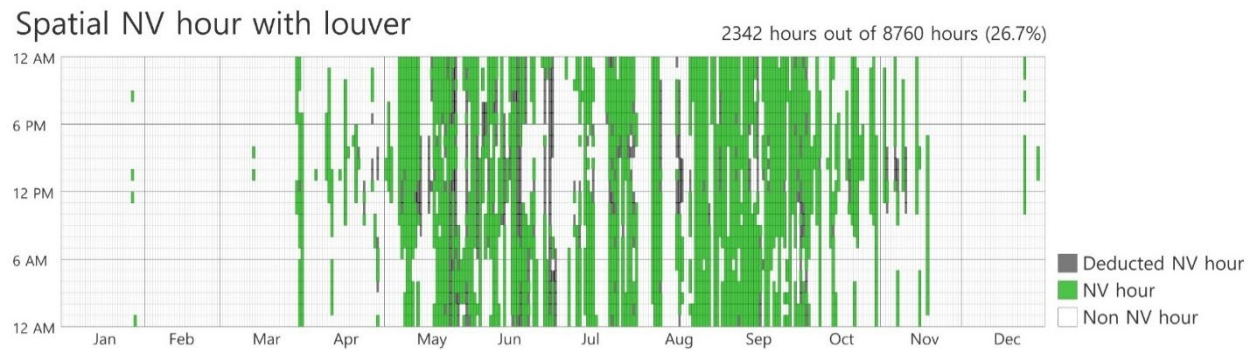
Figure 32: The Spatial NV hour chart with the use of louver visualized in the Rhinoceros viewport

Consequently, the Spatial NV hour chart tells users when NV is available more accurately in a specific space than the Regional NV hour chart. Furthermore, by comparing two charts, users can recognize the effect of utilizing the louvers.

In case energy simulation was used, the cooling load is recalculated. During the NV hours, sensible cooling energy is replaced to zero. Annual cooling load per unit area results by cases are drawn in a graph in the Rhinoceros viewport as in Figure 33. The graphs are drawn in order of a whole year air conditioning case, regional NV hour based case, spatial NV hour based case without the use of louvers, and spatial NV hour based case with the use of louvers. By analyzing the graphs, users can find energy-saving amount when using NV and the louvers.
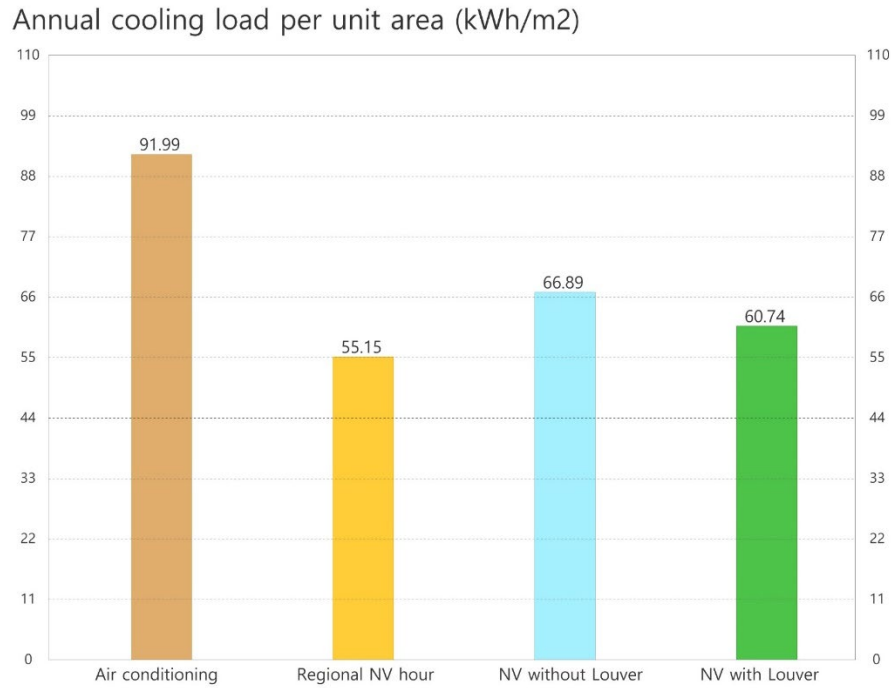
Figure 33: The Annual cooling load per unit area graph visualized in the Rhinoceros viewport

Finally, the hourly control command for the louvers is calculated for 8,760 hours in a typical year. According to the NV conditions, the louvers are commanded to move their axis location and change the opening angle. At the Time select components, users can select a specific hour and check the louver control command as in Figure 34. Concurrently, the operation of the louver is visualized in the Rhinoceros viewport as in Figure 35.
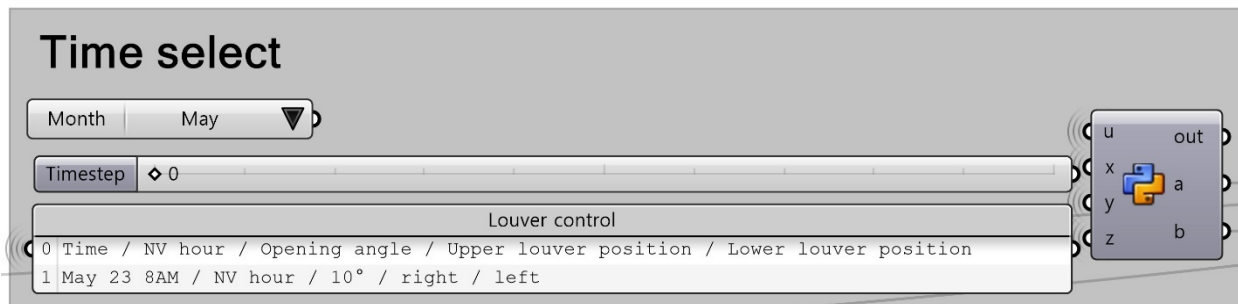
Figure 34: Time select components in Grasshopper canvas
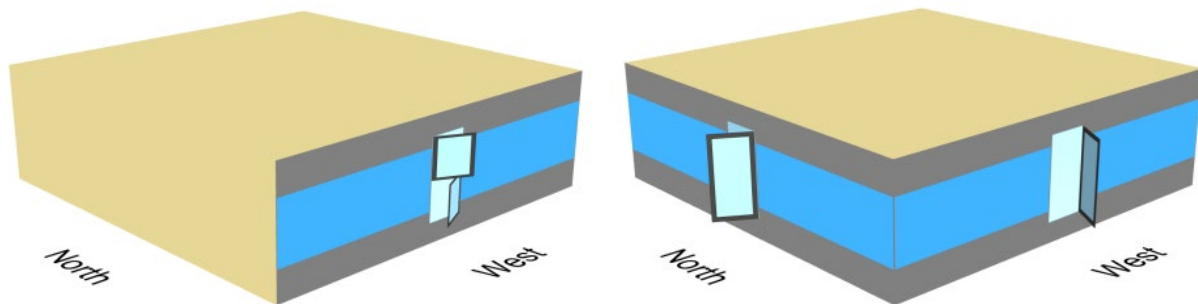
Figure 35: Louver operation visualized in Rhinoceros viewport (single-sided ventilation case-left, cross ventilation case-right)

In conclusion, the simulation tool effectively tests and quantifies extra NV potential and cooling energy-saving potential brought by the louvers.

3. CASE STUDY

By utilizing the simulation tool developed, the automated multi-angle ventilation louver was tested in three different climates and building settings to understand better the louvers' effect on NV potential and cooling load. Three different locations were selected based on the climate zone classifications according to ASHRAE Standard 9.01-2016. Chicago is representing a cool and humid climate (5A), Miami representing a very hot and humid climate (1A), and Los Angeles representing a warm and marine climate (3C). Additionally, each case was assigned to different terrain types, elevation, building program, space program, window to wall ratio (WWR), and target air changes per hour (ACH) setting, as shown in Table 9. The WWR was set to 40% following base envelope design specification in ASHRAE Standard 9.01-2016. The target ACH was set to the numbers assuming user preference in each specific space.

Table 9: Simulation settings

	Wind profile terrain category	Zone elevation (m)	Building program	Space program	WWR (%)	Target ACH
Chicago	Large city centers	30	Large office	Open office	40	3
Miami	Urban and Sub-urban	20	Hospital	Patient room	40	5
Los Angeles	Large city centers	40	High-rise apartment	Apartment	40	2

3.1 Chicago case

The TMY3-based EPW weather data of Chicago was loaded to evaluate the regional NV potential and wind frequency during NV hours. Figure 36 shows the annual regional NV hours

chart of Chicago, a total of 2,608 hours out of the 8,760 hours in a typical year which is

approximately 29.8% of the entire year.
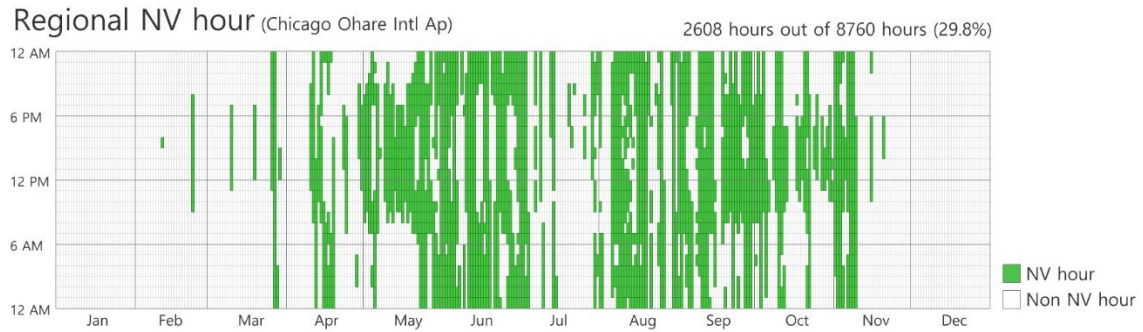
Figure 36: Regional NV hours chart of Chicago

Next, Figure 37 shows the wind frequency during NV hours of Chicago. Approximately 19% of

the wind is the south wind, and approximately 16% of the wind is the northeast wind.
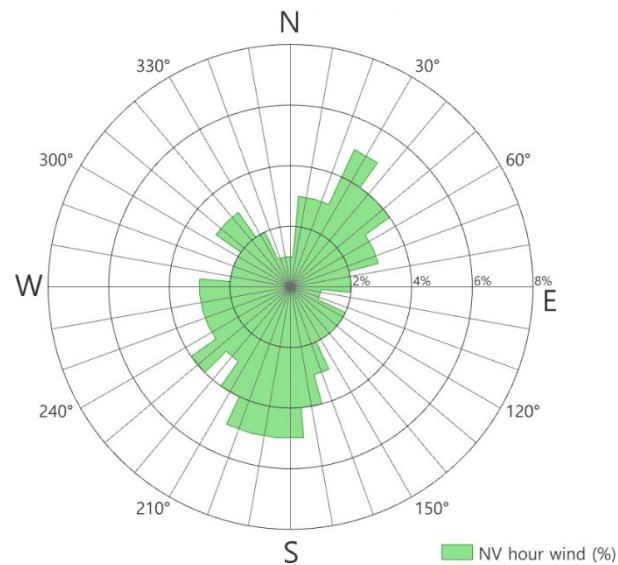
Figure 37: Wind frequency diagram during NV hours of Chicago

3.2.1 Single-sided ventilation

In this section, the single-sided ventilation case for Chicago was developed and analyzed. Targeting to accommodate maximum hours of wind that enables substantial airflow, the opening was set to face south at 190°. The visualization of geometry and defined settings are shown in Figure 38.
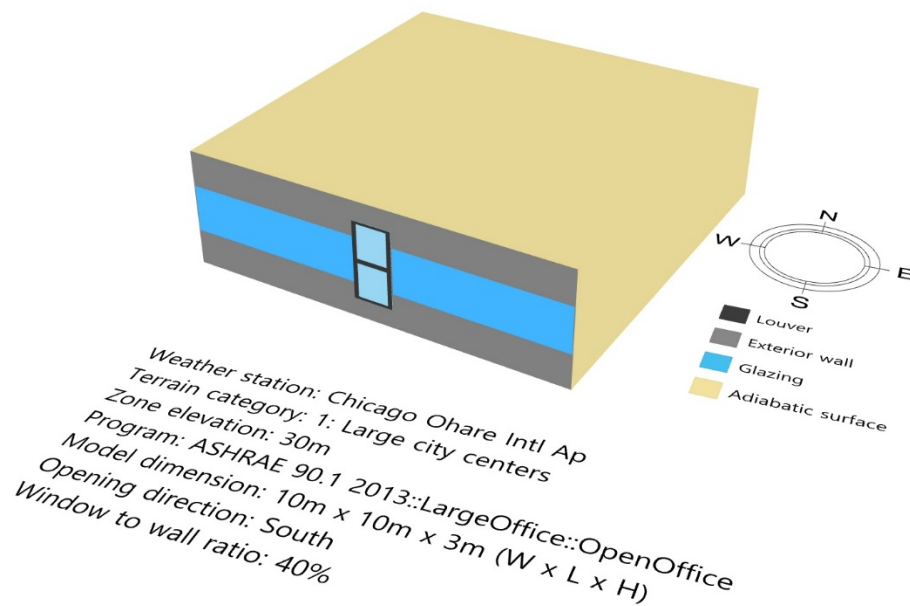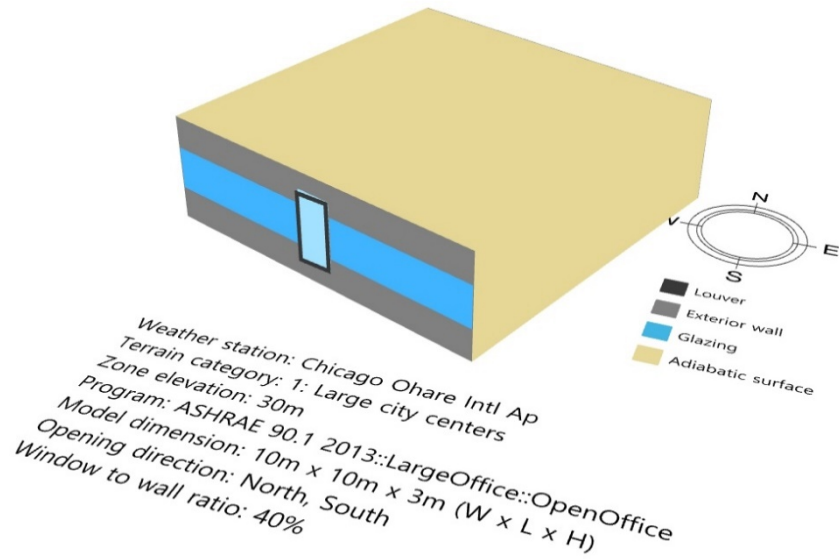

Figure 38: Geometry visualization of Chicago single-sided ventilation case

The mean airflow diagram is visualized as in Figure 39. The blue region, representing mean airflow in the case of opening with the louver, provides significantly larger airflow from entire wind directions compared to the case of opening without the louver. However, the airflow is limited for both cases in northwest, north, and northeast wind hours.
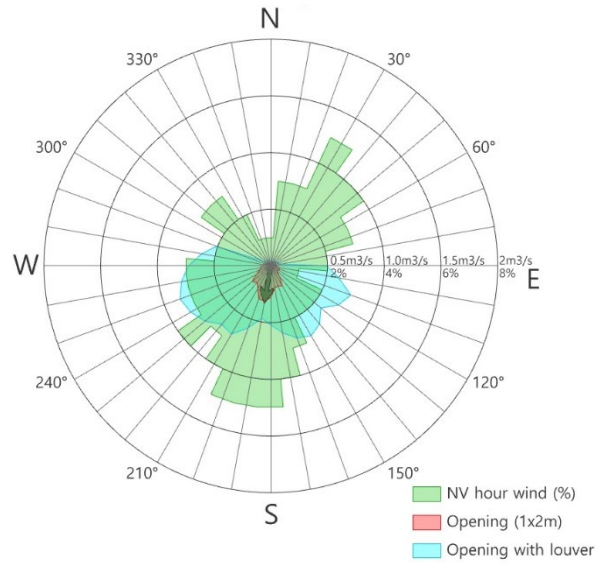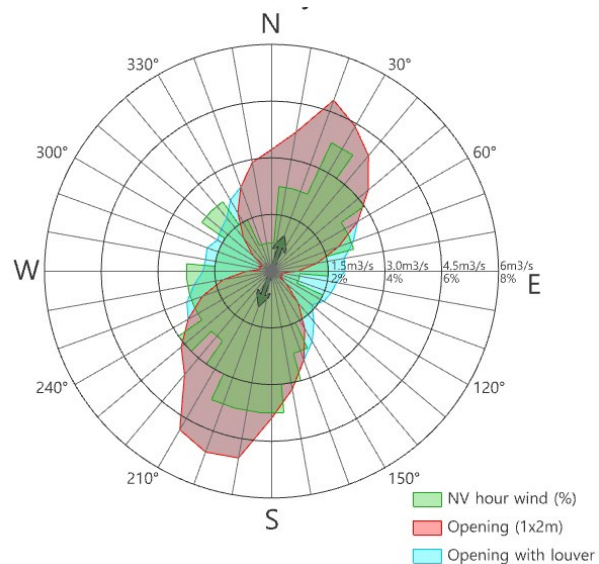
Figure 39: Mean airflow diagram of Chicago single-sided ventilation case

Next, target ACH was set to three, and OpenStudio energy simulation was run to calculate the required airflow. The simulation tool distinguished spatial NV hours and non-spatial NV hours based on required airflow and actual airflow amount each hour.

Figure 40 shows the spatial NV hours chart of the single-sided ventilation without the louver case. Total 1,202 hours out of 8,760 hours (13.7%) were determined to be spatial NV hours showing 1,406 hours of deduction (-53.9%) compared to regional NV hours.
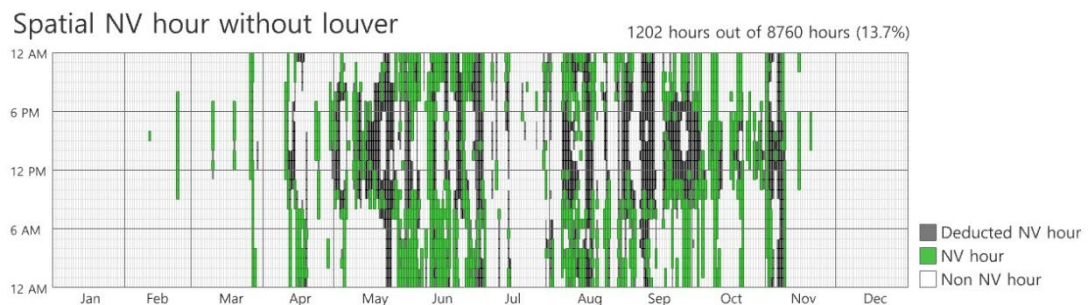
Figure 40: Spatial NV hours chart of Chicago single-sided ventilation without the louver case

Figure 41 shows the spatial NV hours chart of the single-sided ventilation with the louver case.

Total 1,793 hours out of 8,760 hours (20.5%) were determined to be spatial NV hours showing

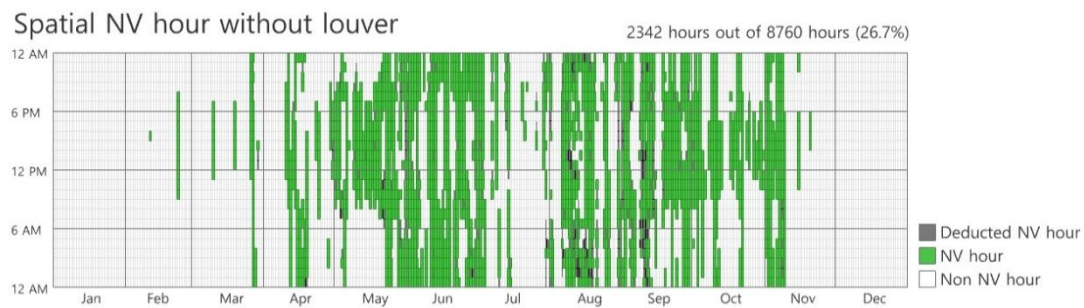815 hours of deduction (-31.3%) compared to regional NV hours. Consequently, natural

ventilation could be utilized for 591 hours more per year if the louver is equipped.
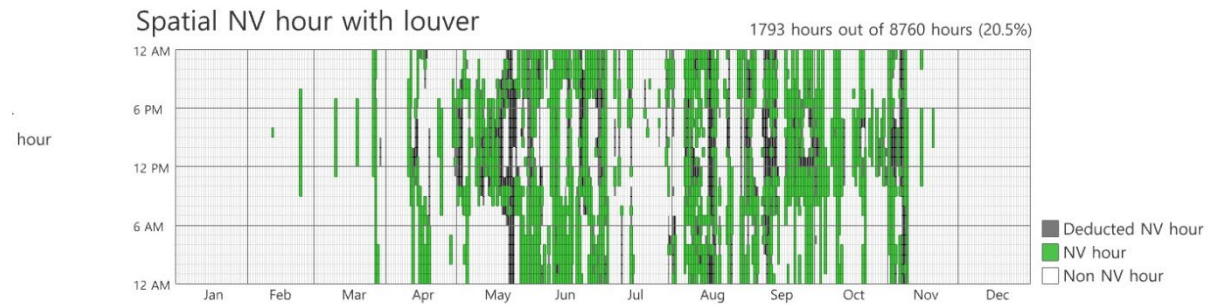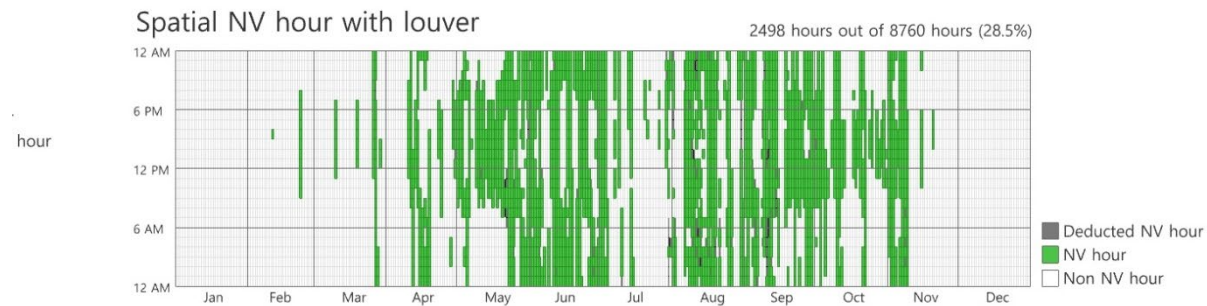

Figure 41: Spatial NV hours chart of Chicago single-sided ventilation with the louver case

Finally, cooling load saving amount was examined. Figure 42 illustrates the amount of annual

cooling load per square meter by cases. The single-sided ventilation without the louver case has

shown 79.48 kWh/m^2 of annual cooling load and 10.46 kWh/m^2 saving compared to the air

conditioning case. On the other hand, the single-sided ventilation with the louver case has shown

73.03 kWh/m^2 of annual cooling load and 16.91 kWh/m^2 saving compared to the air

conditioning case. Therefore, the amount of saving was 61.7% greater if the louver is equipped.
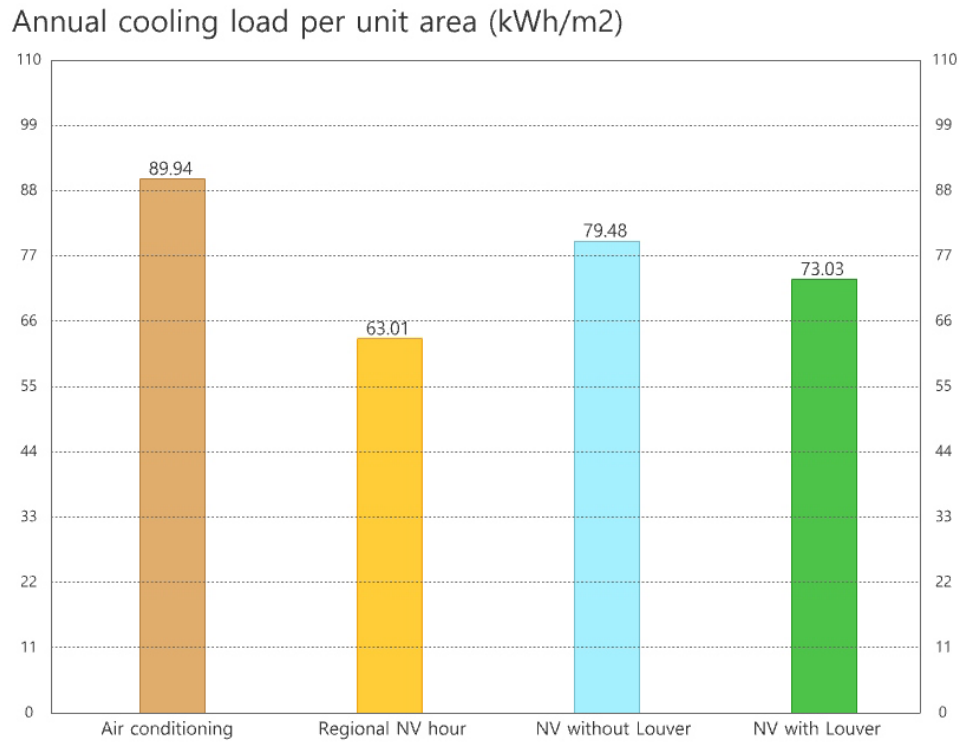
Figure 42: Annual cooling load per unit area of Chicago single-sided ventilation cases

3.2.2 Cross ventilation

Following the single-sided ventilation case, the cross ventilation case for Chicago was developed and analyzed. Targeting to accommodate maximum hours of wind that enables substantial airflow, one opening was set to face north at 20° and another opening was set to face at south at 190°. The visualization of geometry and defined settings are shown in Figure 43.

Figure 43: Geometry visualization of Chicago cross ventilation case

The mean airflow diagram is visualized as in Figure 44. The blue region, representing mean airflow in the case of opening with the louver, provides larger airflow from west and east wind directions compared to the case of opening without the louver.

Figure 44: Mean airflow diagram of Chicago cross ventilation case

Next, target ACH was set to three, and OpenStudio energy simulation was run to calculate the required airflow. The simulation tool distinguished spatial NV hours and non-spatial NV hours based on required airflow and actual airflow amount each hour.

Figure 45 shows the spatial NV hours chart of the cross ventilation without the louver case. Total 2,342 hours out of 8,760 hours (26.7%) were determined to be spatial NV hours showing 266 hours of deduction (-10.2%) compared to regional NV hours.

Figure 45: Spatial NV hours chart of Chicago cross ventilation without the louver case

Figure 46 shows the spatial NV hours chart of the cross ventilation with the louver case. Total 2,498 hours out of 8,760 hours (28.5%) were determined to be spatial NV hours showing 110 hours of deduction (-4.4%) compared to regional NV hours. Consequently, natural ventilation could be utilized for 156 hours more per year if the louver is equipped.

Figure 46: Spatial NV hours chart of Chicago cross ventilation with the louver case

Finally, cooling load saving amount was examined. Figure 47 illustrates the amount of annual cooling load per square meter by cases. The cross ventilation without the louver case has shown 54.48 kWh/m^2 of annual cooling load and 24.28 kWh/m^2 saving compared to the air conditioning case. On the other hand, the cross ventilation with the louver case has shown 53.1 kWh/m^2 of annual cooling load and 25.66 kWh/m^2 saving compared to the air conditioning case. Therefore, the amount of saving was 5.7% greater if the louver is equipped.
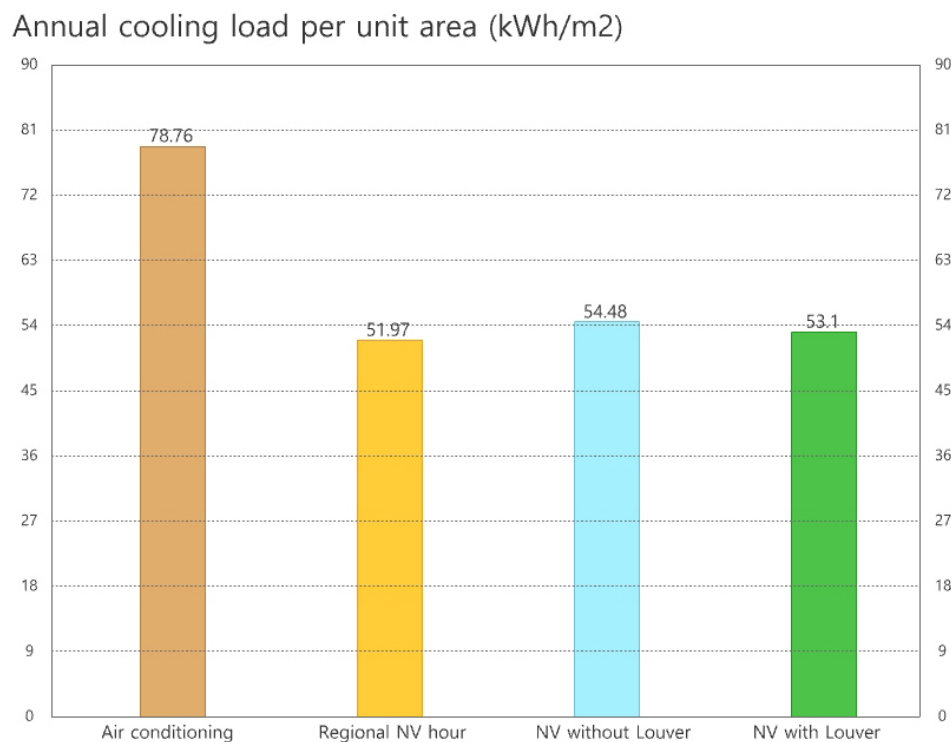
Figure 47: Annual cooling load per unit area of Chicago cross ventilation cases

3.2 Miami case

Next, the TMY3-based EPW weather data of Miami was loaded to evaluate the regional NV potential and wind frequency during NV hours. Figure 48 shows the annual regional NV hours

chart of Miami, a total of 1,906 hours out of the 8,760 hours in a typical year which is

approximately 21.8% of the entire year.
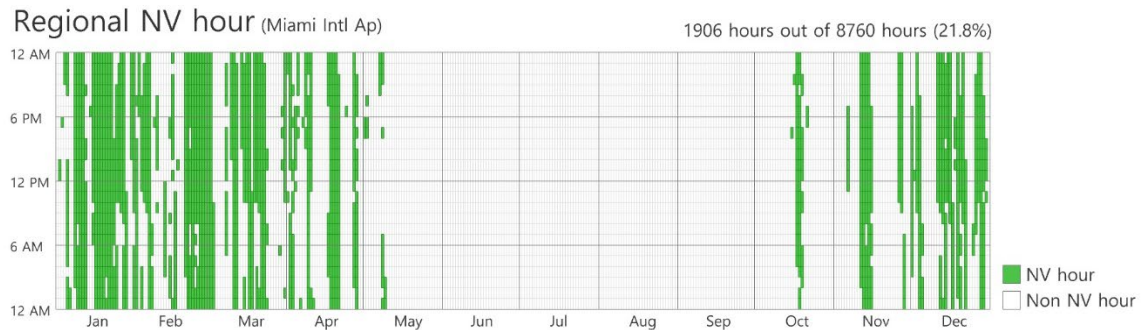
Figure 48: Regional NV hours chart of Miami

Next, Figure 49 shows the wind frequency during NV hours of Miami. Approximately 35% of the

wind is the northwest wind, and approximately 26% of the wind is the east wind.
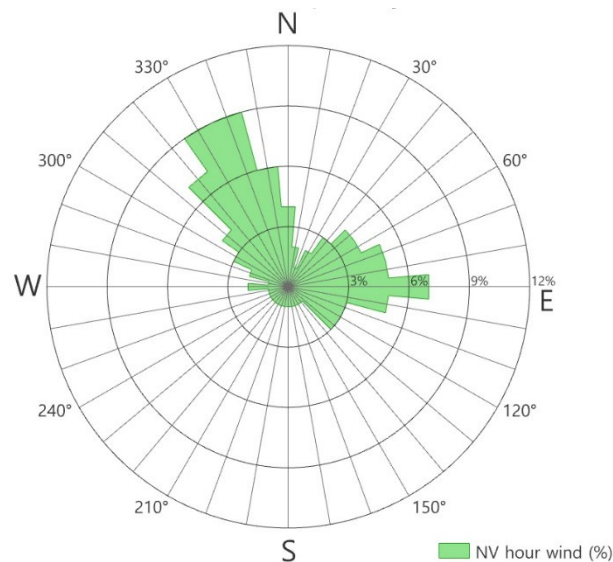
Figure 49: Wind frequency diagram during NV hours of Miami

3.2.1 Single-sided ventilation

In this section, the single-sided ventilation case for Miami was developed and analyzed.

Targeting to accommodate maximum hours of wind that enables substantial airflow, the opening

was set to face north at 20°. The visualization of geometry and defined settings are shown in

Figure 50.
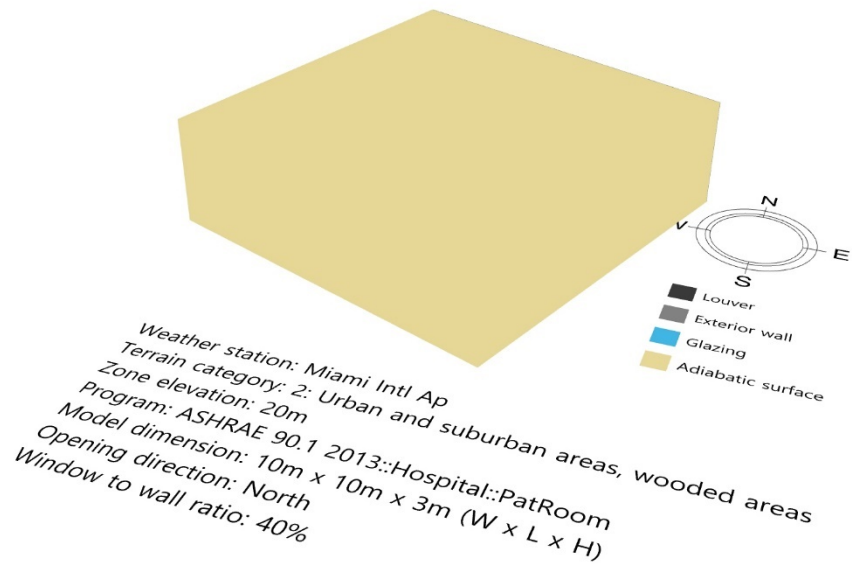
Figure 50: Geometry visualization of Miami single-sided ventilation case

The mean airflow diagram is visualized as in Figure 51. The blue region, representing mean

airflow in the case of opening with the louver, provides significantly larger airflow from entire

wind directions compared to the case of opening without the louver.
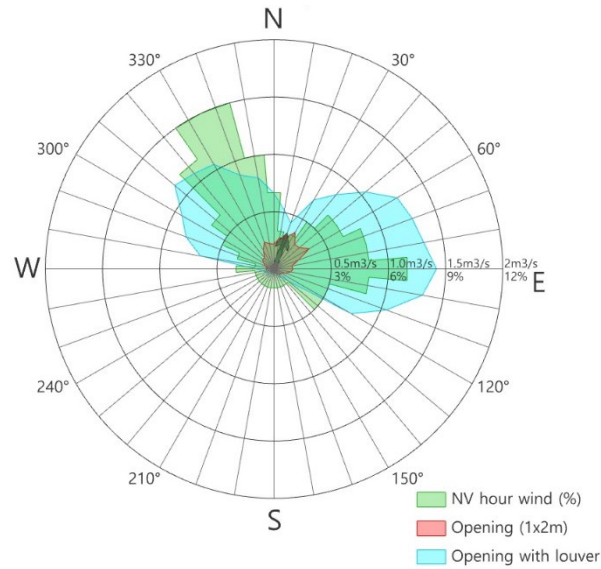
Figure 51: Mean airflow diagram of Miami single-sided ventilation case

Next, target ACH was set to five, and OpenStudio energy simulation was run to calculate the required airflow. The simulation tool distinguished spatial NV hours and non-spatial NV hours based on required airflow and actual airflow amount each hour.

Figure 52 shows the spatial NV hours chart of the single-sided ventilation without the louver case. Total 83 hours out of 8,760 hours (0.9%) were determined to be spatial NV hours showing 1,823 hours of deduction (-95.6%) compared to regional NV hours.
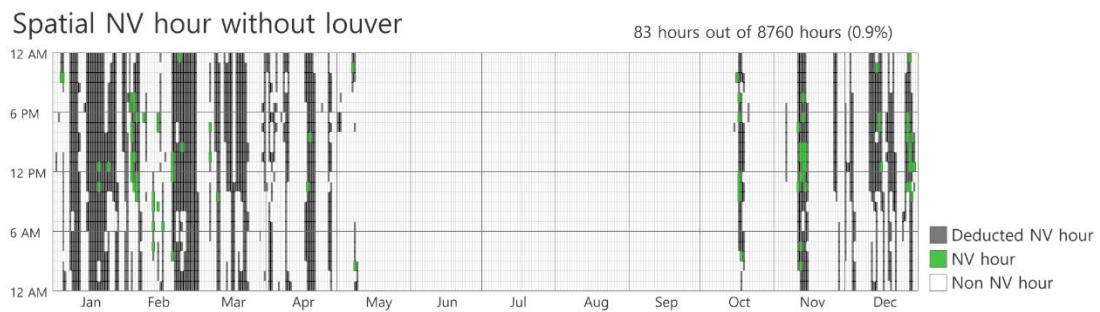
Figure 52: Spatial NV hours chart of Miami single-sided ventilation without the louver case

Figure 53 shows the spatial NV hours chart of the single-sided ventilation with the louver case. Total 1,473 hours out of 8,760 hours (16.8%) were determined to be spatial NV hours showing 433 hours of deduction (-22.7%) compared to regional NV hours. Consequently, natural ventilation could be utilized for 1,390 hours more per year if the louver is equipped.
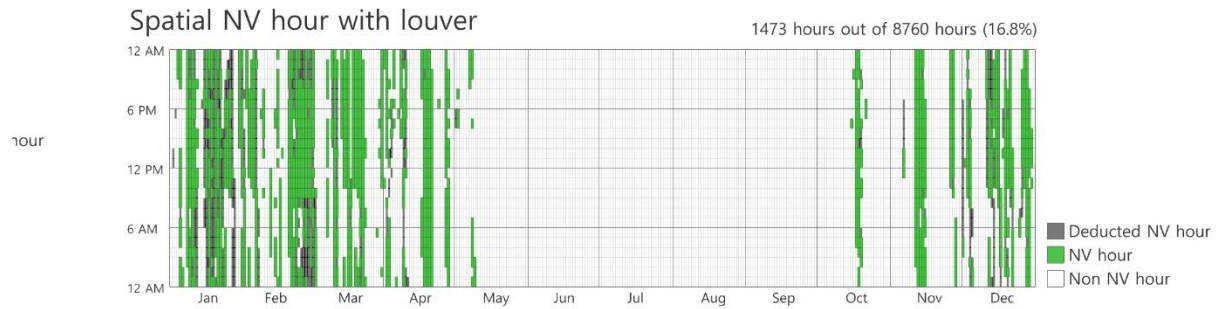
Figure 53: Spatial NV hours chart of Miami single-sided ventilation with the louver case

Finally, cooling load saving amount was examined. Figure 54 illustrates the amount of annual cooling load per square meter by cases. The single-sided ventilation without the louver case has shown 198.08 kWh/m² of annual cooling load and 4.14 kWh/m² saving compared to the air conditioning case. On the other hand, the single-sided ventilation with the louver case has shown 175.21 kWh/m² of annual cooling load and 27.01 kWh/m² saving compared to the air conditioning case. Therefore, the amount of saving was 652.4% greater if the louver is equipped.

Annual cooling load per unit area (kWh/m2)
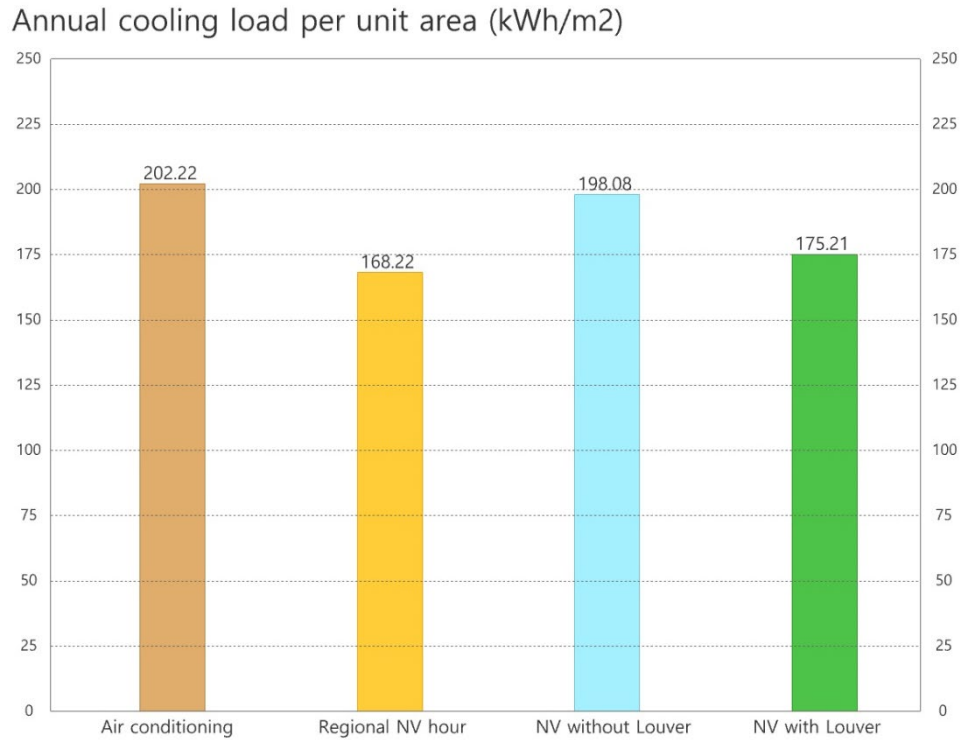
Figure 54: Annual cooling load per unit area of Miami single-sided ventilation cases

3.2.2 Cross ventilation

Following the single-sided ventilation case, the cross ventilation case for Miami was developed and analyzed. Targeting to accommodate maximum hours of wind that enables substantial airflow, one opening was set to face north at 340° and another opening was set to face at east at 70°. The visualization of geometry and defined settings are shown in Figure 55.
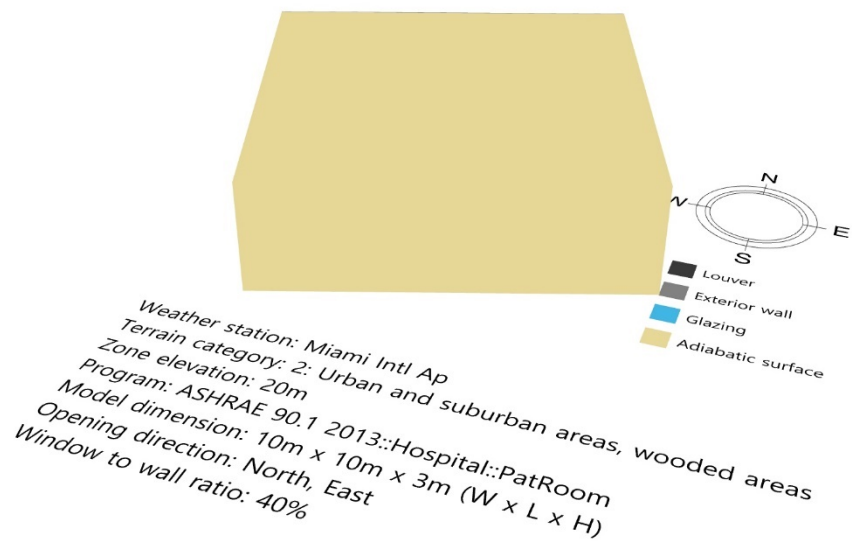
Weather station: Miami Intl Ap
Terrain category: 2: Urban and suburban areas, wooded areas
Zone elevation: 20m
Program: ASHRAE 90.1 2013::Hospital::PatRoom
Model dimension: 10m x 10m x 3m (W x L x H)
Opening direction: North, East
Window to wall ratio: 40%

Louver
Exterior wall
Glazing
Adiabatic surface

Figure 55: Geometry visualization of Miami cross ventilation case

The mean airflow diagram is visualized as in Figure 56. The blue region, representing mean airflow in the case of opening with the louver, provides larger airflow from west, north and southeast wind directions compared to the case of opening without the louver.

NV hour wind (%)
Opening (1x2m)
Opening with louver
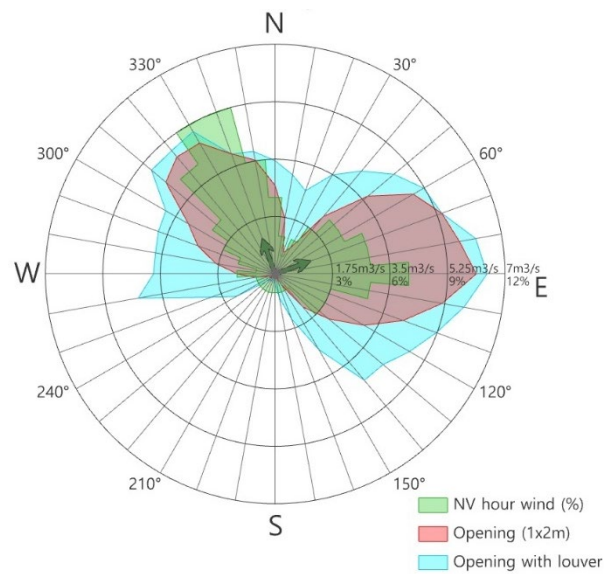
Figure 56: Mean airflow diagram of Miami cross ventilation case

Next, target ACH was set to five, and OpenStudio energy simulation was run to calculate the required airflow. The simulation tool distinguished spatial NV hours and non-spatial NV hours based on required airflow and actual airflow amount each hour.

Figure 57 shows the spatial NV hours chart of the cross ventilation without the louver case. Total 1,703 hours out of 8,760 hours (19.4%) were determined to be spatial NV hours showing 203 hours of deduction (-10.7%) compared to regional NV hours.

Figure 57: Spatial NV hours chart of Miami cross ventilation without the louver case

Figure 58 shows the spatial NV hours chart of the cross ventilation with the louver case. Total 1,758 hours out of 8,760 hours (20.1%) were determined to be spatial NV hours showing 148 hours of deduction (-7.8%) compared to regional NV hours. Consequently, natural ventilation could be utilized for 55 hours more per year if the louver is equipped.

Figure 58: Spatial NV hours chart of Miami cross ventilation with the louver case

Finally, cooling load saving amount was examined. Figure 59 illustrates the amount of annual cooling load per square meter by cases. The cross ventilation without the louver case has shown 196.52 kWh/m² of annual cooling load and 31.85 kWh/m² saving compared to the air conditioning case. On the other hand, the cross ventilation with the louver case has shown 195.75 kWh/m² of annual cooling load and 32.62 kWh/m² saving compared to the air conditioning case. Therefore, the amount of saving was 2.4% greater if the louver is equipped.
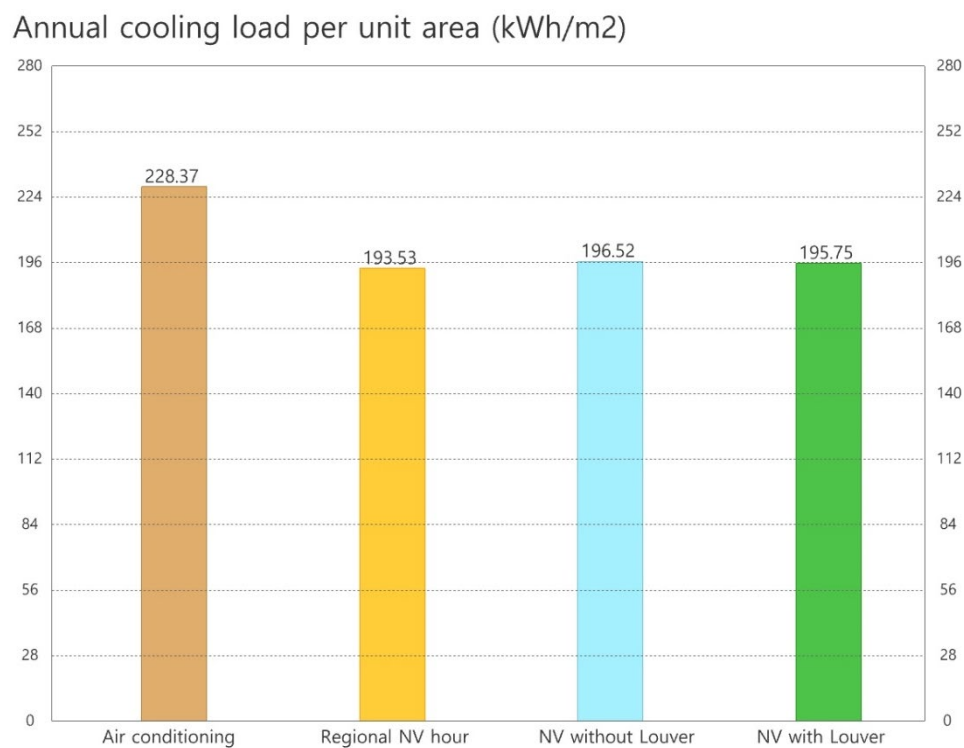
Figure 59: Annual cooling load per unit area of Miami cross ventilation cases

3.3 Los Angeles case

Finally, the TMY3-based EPW weather data of Los Angeles was loaded to evaluate the regional NV potential and wind frequency during NV hours. Figure 60 shows the annual regional NV

hours chart of Los Angeles, a total of 6,706 hours out of the 8,760 hours in a typical year which

is approximately 76.6% of the entire year.
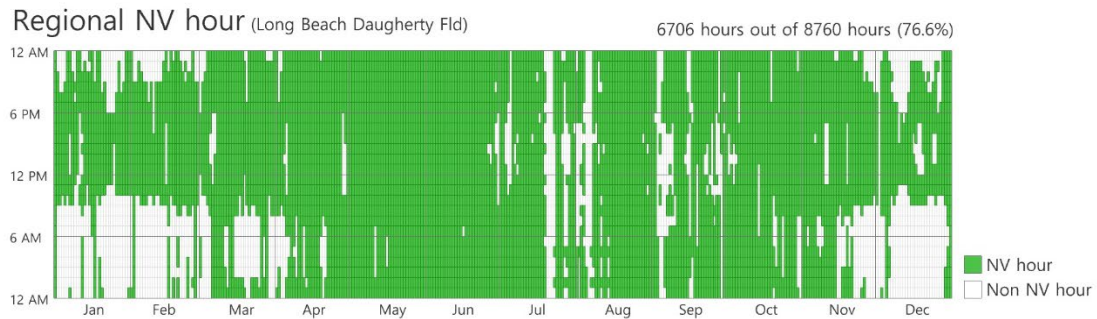
Figure 60: Regional NV hours chart of Los Angeles

Next, Figure 61 shows the wind frequency during NV hours of Los Angeles. Approximately 23%

of the wind is the northwest wind, and approximately 23% of the wind is the south wind.
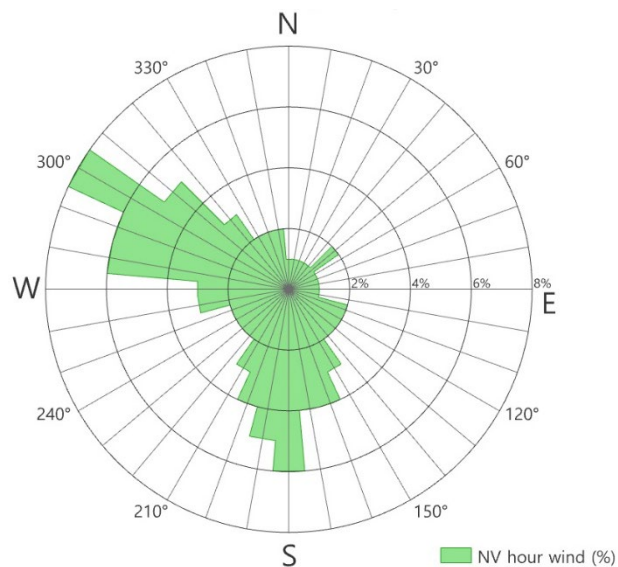

Figure 61: Wind frequency diagram during NV hours of Los Angeles

3.2.1 Single-sided ventilation

In this section, the single-sided ventilation case for Los Angeles was developed and analyzed. Targeting to accommodate maximum hours of wind that enables substantial airflow, the opening was set to face west at 250°. The visualization of geometry and defined settings are shown in Figure 62.
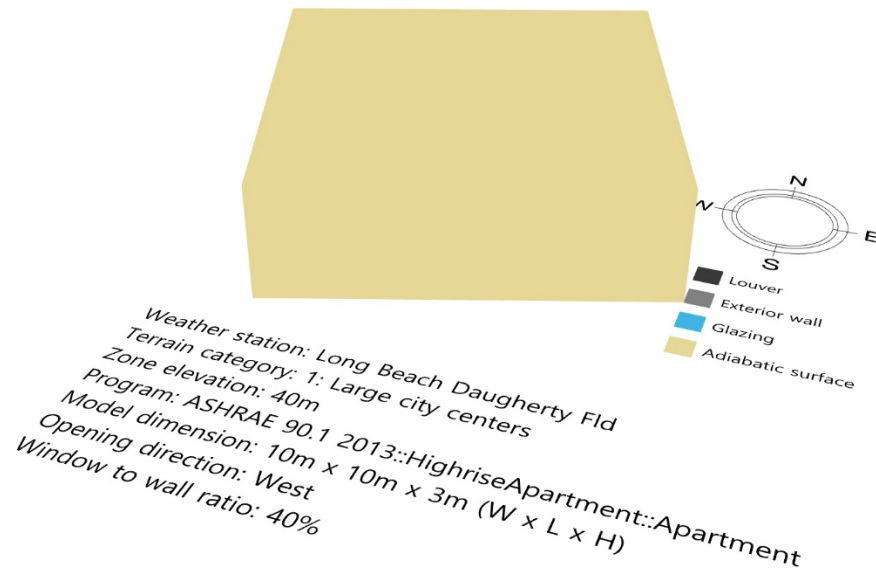
Figure 62: Geometry visualization of Los Angeles single-sided ventilation case

The mean airflow diagram is visualized as in Figure 63. The blue region, representing mean airflow in the case of opening with the louver, provides significantly larger airflow from entire wind directions compared to the case of opening without the louver.
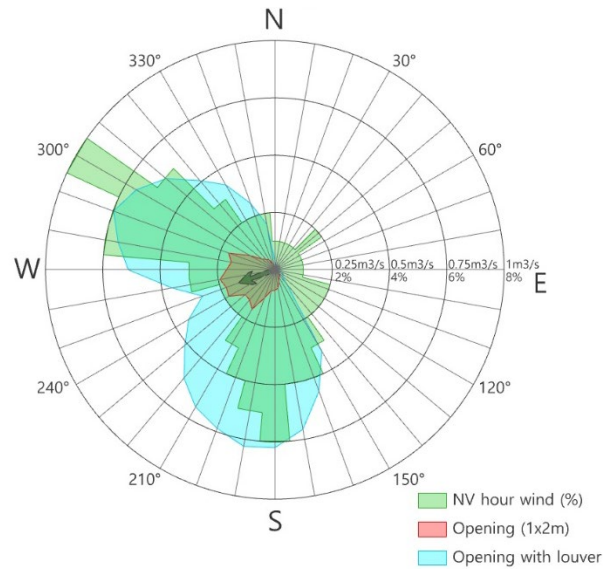
Figure 63: Mean airflow diagram of Los Angeles single-sided ventilation case

Next, target ACH was set to two, and OpenStudio energy simulation was run to calculate the required airflow. The simulation tool distinguished spatial NV hours and non-spatial NV hours based on required airflow and actual airflow amount each hour.

Figure 64 shows the spatial NV hours chart of the single-sided ventilation without the louver case. Total 1,132 hours out of 8,760 hours (12.9%) were determined to be spatial NV hours showing 5,574 hours of deduction (-83.1%) compared to regional NV hours.
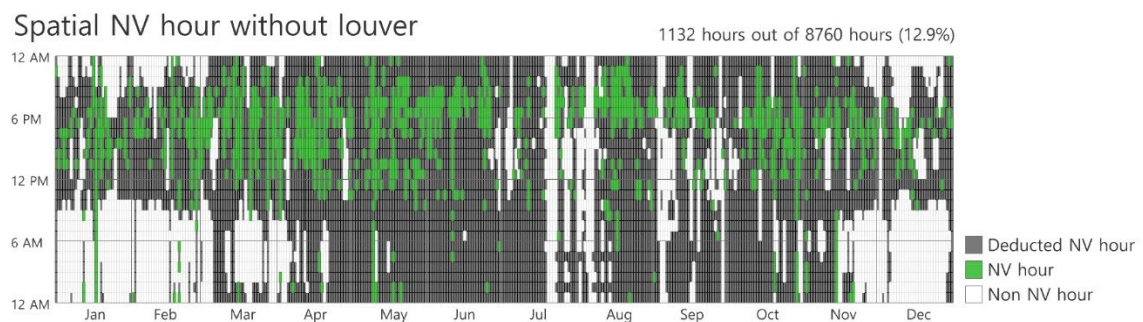

Figure 64: Spatial NV hours chart of Los Angeles single-sided ventilation without the louver case

Figure 65 shows the spatial NV hours chart of the single-sided ventilation with the louver case. Total 4,603 hours out of 8,760 hours (52.5%) were determined to be spatial NV hours showing 2,103 hours of deduction (-31.4%) compared to regional NV hours. Consequently, natural ventilation could be utilized for 3,471 hours more per year if the louver is equipped.
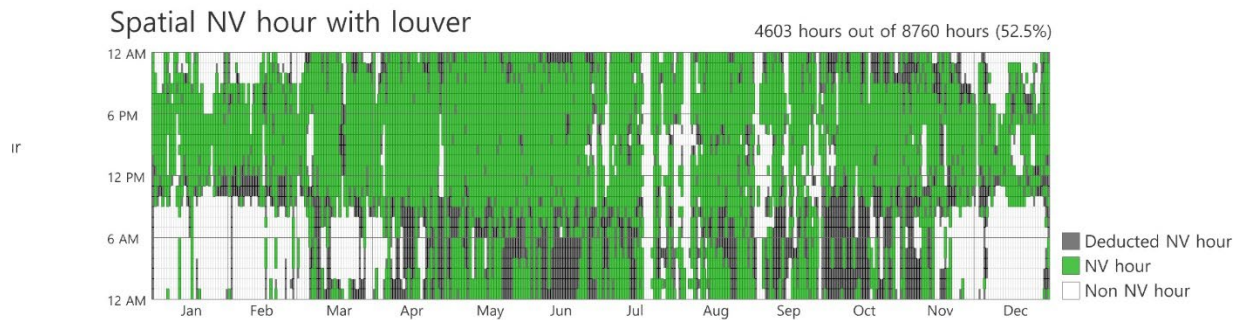

Figure 65: Spatial NV hours chart of Los Angeles single-sided ventilation with the louver case

Finally, cooling load saving amount was examined. Figure 66 illustrates the amount of annual cooling load per square meter by cases. The single-sided ventilation without the louver case has shown 65.22 kWh/m² of annual cooling load and 20.97 kWh/m² saving compared to the air conditioning case. On the other hand, the single-sided ventilation with the louver case has shown 35.02 kWh/m² of annual cooling load and 51.17 kWh/m² saving compared to the air conditioning case. Therefore, the amount of saving was 244.0% greater if the louver is equipped.
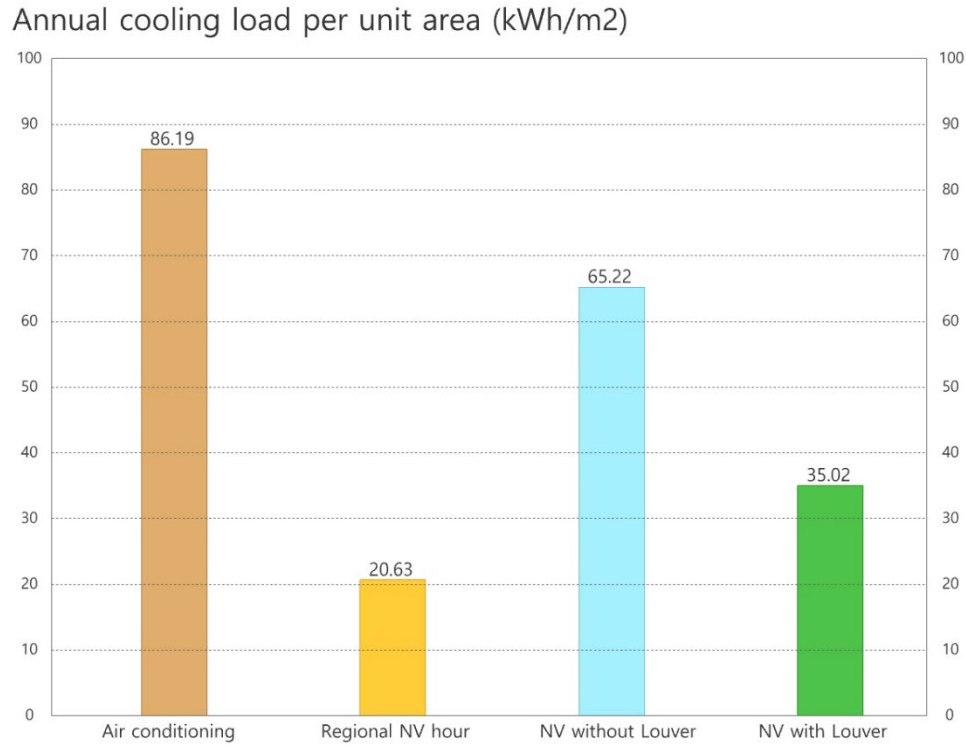
Figure 66: Annual cooling load per unit area of Los Angeles single-sided ventilation cases

3.2.2 Cross ventilation

Following the single-sided ventilation case, the cross ventilation case for Los Angeles was developed and analyzed. Targeting to accommodate maximum hours of wind that enables substantial airflow, one opening was set to face south at 190° and another opening was set to face at west at 280°. The visualization of geometry and defined settings are shown in Figure 67.
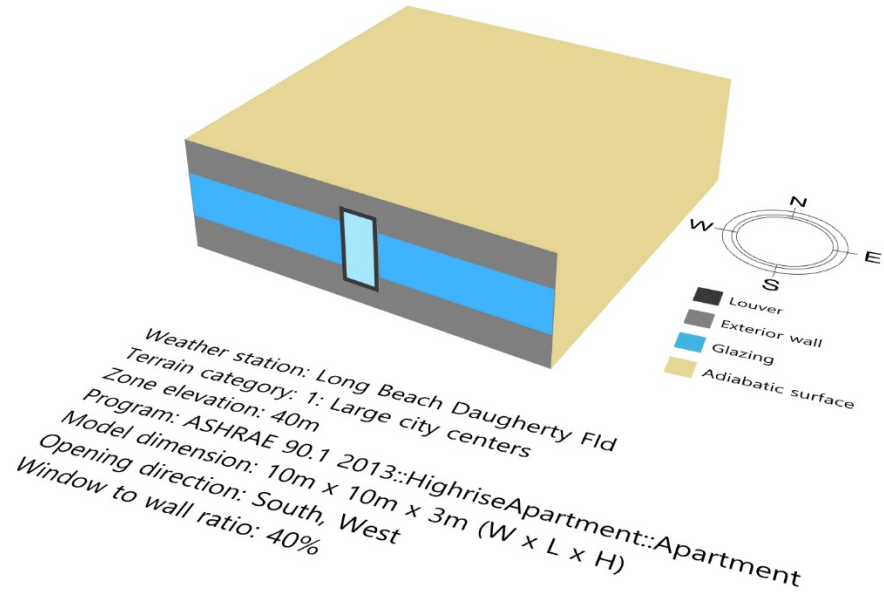
Weather station: Long Beach Daugherty Fld
Terrain category: 1: Large city centers
Zone elevation: 40m
Program: ASHRAE 90.1 2013::HighriseApartment::Apartment
Model dimension: 10m x 10m x 3m (W x L x H)
Opening direction: South, West
Window to wall ratio: 40%

Figure 67: Geometry visualization of Los Angeles cross ventilation case

The mean airflow diagram is visualized as in Figure 68. The blue region, representing mean airflow in the case of opening with the louver, provides larger airflow from southwest wind directions compared to the case of opening without the louver.
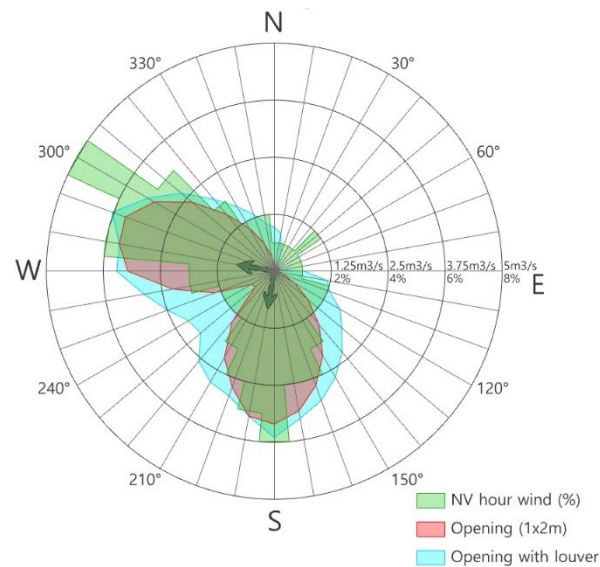

Figure 68: Mean airflow diagram of Los Angeles cross ventilation case

Next, target ACH was set to two, and OpenStudio energy simulation was run to calculate the required airflow. The simulation tool distinguished spatial NV hours and non-spatial NV hours based on required airflow and actual airflow amount each hour.

Figure 69 shows the spatial NV hours chart of the cross ventilation without the louver case. Total 5,301 hours out of 8,760 hours (60.5%) were determined to be spatial NV hours showing 1,405 hours of deduction (-20.6%) compared to regional NV hours.
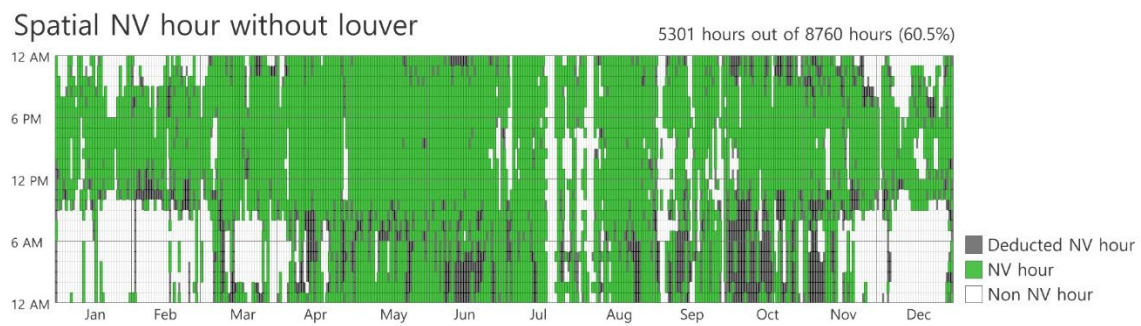

Figure 69: Spatial NV hours chart of Los Angeles cross ventilation without the louver case

Figure 70 shows the spatial NV hours chart of the cross ventilation with the louver case. Total 5,748 hours out of 8,760 hours (65.6%) were determined to be spatial NV hours showing 958 hours of deduction (-14.3%) compared to regional NV hours. Consequently, natural ventilation could be utilized for 447 hours more per year if the louver is equipped.
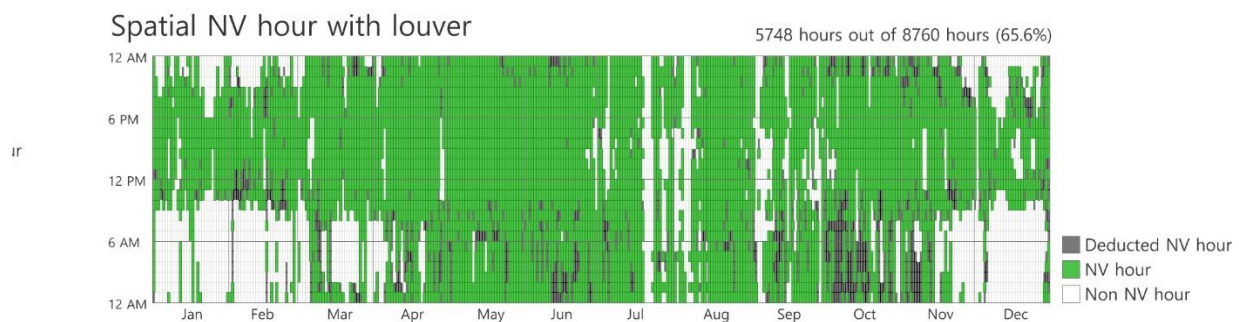

Figure 70: Spatial NV hours chart of Los Angeles cross ventilation with the louver case

Finally, cooling load saving amount was examined. Figure 71 illustrates the amount of annual cooling load per square meter by cases. The cross ventilation without the louver case has shown 26.51 kWh/m^2 of annual cooling load and 55.76 kWh/m^2 saving compared to the air conditioning case. On the other hand, the cross ventilation with the louver case has shown 23.98 kWh/m^2 of annual cooling load and 58.29 kWh/m^2 saving compared to the air conditioning case. Therefore, the amount of saving was 4.5% greater if the louver is equipped.
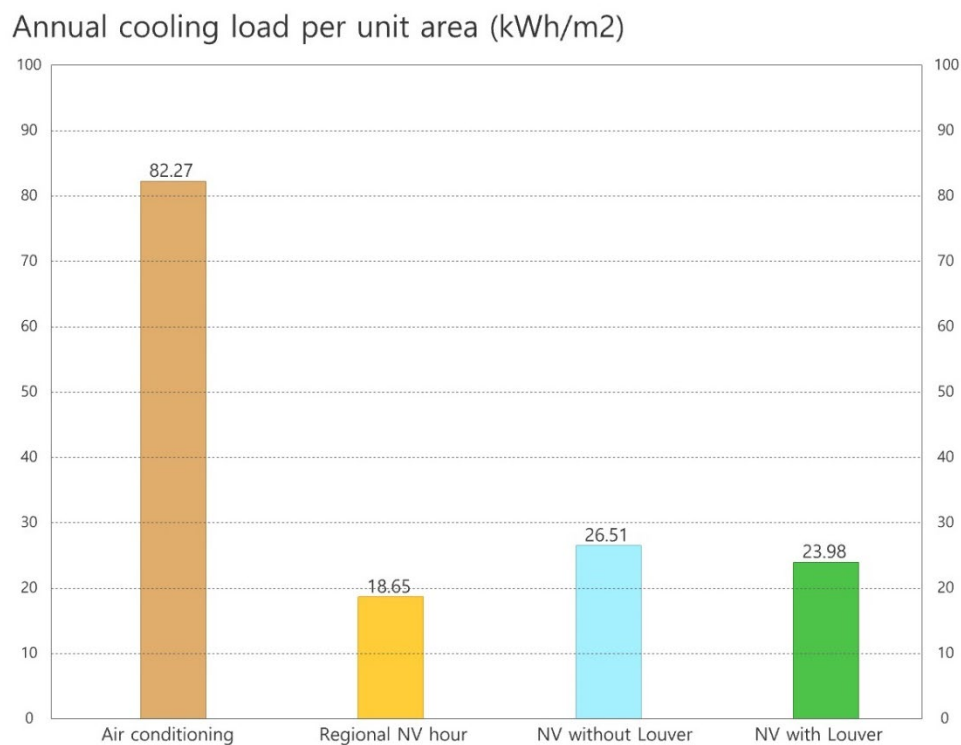

Figure 71: Annual cooling load per unit area of Los Angeles cross ventilation cases

3.4 Case study summary

This section summarizes the results from case studies conducted. Each case examined the effects of louvers in NV potential and cooling energy-saving potential located in different climates. Table 10 summarizes the case study results.

Table 10: Case study results

Location	Method		NV hours (hours)	Cooling load (kWh/m²)
Chicago	Single-sided ventilation	Regional	2,608	63.01
		Without louver	1,202	79.48
		With louver	1,793	73.03
	Cross ventilation	Regional	2,608	51.97
		Without louver	2,342	54.48
		With louver	2,498	53.1
Miami	Single-sided ventilation	Regional	1,906	168.22
		Without louver	83	198.08
		With louver	1,473	175.21
	Cross ventilation	Regional	1,906	193.53
		Without louver	1,703	196.52
		With louver	1,758	195.75
Los Angeles	Single-sided ventilation	Regional	6,706	20.63
		Without louver	1,132	65.22
		With louver	4,603	35.02
	Cross ventilation	Regional	6,706	18.65
		Without louver	5,301	26.51
		With louver	5,748	23.98

In general, the louvers provided a higher effect on both NV potential and cooling energy-saving potential on single-sided ventilation cases compared to cross ventilation cases. Since the louver on a single-sided opening brought significantly higher airflow compared to an opening without the louver, required airflow was easily fulfilled and eventually brought significantly higher NV potential and cooling energy-saving potential. On the other hand, cross ventilation cases have shown less differences in NV potential and cooling energy-saving potential than single-sided ventilation cases. The difference was smaller since extra airflow available by utilizing the louvers was not significant in cross ventilation. However, the case studies have set the opening directions facing frequent wind directions. As the louvers enable bringing airflow from a broader range of wind, if the openings are set facing far from the frequent wind directions, the effect of utilizing the louvers could become higher.

4. DISCUSSION

This section evaluates the findings of this research, states the limitations, and propose possible future studies.

4.1 Evaluation of the louver design

This proposed idea of utilizing the louvers for higher NV potential aims to control the pressure between the inlet and outlet of airflow. The pressure difference is one of the main drivers in the standard orifice flow equation determining airflow into space along with the opening area. Unlike conventional windows, the louvers are designed to move their axis horizontally and control their opening angle to control both pressure and opening area.

Despite the effectiveness of the louvers, there are limitations and future works to be done. The shape of the louvers did not consider the aerodynamical design, and the size of the louver unit is fixed to one-meter width and two-meter height. Further development on the shape and size could bring higher NV potential by accommodating higher airflow from a broader range of wind directions.

4.2 Evaluation of the CFD simulation

The CFD simulation was employed to test the effectiveness of the louvers by calculating airflow introduced into space. Three different types of opening configurations were tested. Those are single-sided opening, two openings in opposite directions, and two openings in adjacent directions. The simulations have proven that the openings with the louvers collected higher airflow from a wider range of wind directions in the entire opening types than openings without the louvers.

Nevertheless, the CFD simulation environment was limited to specific setting due to the number of cases to be covered and the time required to run each simulation. The space size was limited to ten-meter on each side and three-meter in height. This may not match the outcome of a simulation on a whole building scale. Next, only one louver was located at the center of each exterior wall. The number and location of louvers may impact simulation and could be deployed by considering prevailing wind direction and space program. Furthermore, the louvers were set to be open to the same angle on each simulation. Opening each louver at different angles causes different opening areas and receives more diverse wind pressure on the openings, resulting in a sophisticated control of NV paths inside the space. Finally, surrounding environments were not accounted in the simulations. Wind patterns are highly affected by adjacent buildings and obstacles.

Stepping further from running a CFD simulation in a restricted model, more flexible methods could be employed to consider various building designs, more dynamic louver control, and surrounding environments. Real-time CFD and machine learning technology can be applied for this step in the future.

4.3 Evaluation of the control system

The control system of the louvers in this study aims to find an optimal position and opening angle of the louvers based on the required airflow for cooling and ventilation.

However, the louvers have further potential to control the path and speed of airflow within the space. A more advanced control system may control the louvers to focus NV on the portion of the space where occupants are congested and maintain the airspeed within the comfort range. Future work might propose a more comprehensive control system for the louvers that can

consider volume, path, and speed of NV utilizing sensor technology, model predictive control, and machine learning.

4.4 Evaluation of the simulation tool

Utilizing the simulation tool, users can investigate NV potential and cooling energy saving potential for various cases. Users may change EnergyPlus weather files, geometry settings, and building programs. Visualization of building geometry, charts, and results are provided step by step to assist users in designing a naturally ventilated building with high potential. Finally, NV potential and cooling energy saving potential are given on a regional scale, spatial scale without the use of louvers, and spatial scale using louvers.

Future work can include the following enhancements. The simulation tool may expand its level of freedom by allowing users to design their building geometry model in the Rhinoceros interface. This includes specifying the number and location of the louvers. Furthermore, a real-time CFD engine will calculate the airflow following the user's building configurations instead of precalculated data to secure the accuracy of the calculation.

5. CONCLUSIONS

This study proposes automated multi-angle ventilation louvers that can control wind pressure around a building and enables higher natural ventilation potential. The louver design targets to achieve high practicality in terms of cost and maintenance. Hardware is minimized, and software is sophisticatedly designed to control the louvers. The effectiveness of louvers was tested by calculating the airflow in CFD simulation. A simple control system for the louvers was designed. A simulation tool was developed in Rhinoceros and Grasshopper interface to analyze the length of the NV period and cooling energy saving amount at specific locations.

In conclusion, this research will facilitate the use of NV for cooling and ventilating the space. Buildings currently using or planning to use NV will further reduce energy consumption and improve indoor environmental quality by the louvers. Buildings in a disadvantageous location for NV in terms of weather conditions or the surrounding environment might gain feasibility in utilizing NV by the louvers.

6. ACKNOWLEDGEMENT

REFERENCES

UN, World Urbanization Prospects: The 2018 Revision, Department of Economic and Social Affairs, United Nations, 2018.

Crawley, D. B. (2008). Estimating the impacts of climate change and urbanization on building performance. *Journal of Building Performance Simulation*, *1*(2), 91-115.

Luo, Z., Zhao, J., Gao, J., & He, L. (2007). Estimating natural-ventilation potential considering both thermal comfort and IAQ issues. *Building and environment*, *42*(6), 2289-2298.

Tong, Z., Chen, Y., Malkawi, A., Liu, Z., & Freeman, R. B. (2016). Energy saving potential of natural ventilation in China: The impact of ambient air pollution. *Applied energy*, *179*, 660-668.

Korsavi, S. S., Montazami, A., & Mumovic, D. (2020). Indoor air quality (IAQ) in naturally-ventilated primary schools in the UK: occupant-related factors. *Building and Environment*, *180*, 106992.

Aynsley, R. (1999). Estimating summer wind driven natural ventilation potential for indoor thermal comfort. *Journal of Wind Engineering and Industrial Aerodynamics*, *83*(1-3), 515-525.

Yao, R., Li, B., Steemers, K., & Short, A. (2009). Assessing the natural ventilation cooling potential of office buildings in different climate zones in China. *Renewable Energy*, *34*(12), 2697-2705.

Cheng, J., Qi, D., Katal, A., Wang, L. L., & Stathopoulos, T. (2018). Evaluating wind-driven natural ventilation potential for early building design. *Journal of Wind Engineering and Industrial Aerodynamics*, *182*, 160-169.

Sakiyama, N. R. M., Mazzaferro, L., Carlo, J. C., Bejat, T., & Garrecht, H. (2021). Natural ventilation potential from weather analyses and building simulation. *Energy and Buildings*, *231*, 110596

Chen, Y., Tong, Z., & Malkawi, A. (2017). Investigating natural ventilation potentials across the globe: Regional and climatic variations. *Building and Environment*, *122*, 386-396.

Wang, B., & Malkawi, A. (2015). Genetic algorithm based building form optimization study for natural ventilation potential. In *BS2015: 14th Conference of International Building Performance Simulation Association*.

Lim, H. S., & Kim, G. (2018). The renovation of window mechanism for natural ventilation in a high-rise residential building. *International Journal of Ventilation*, *17*(1), 17-30.

Yoon, N., Piette, M. A., Han, J. M., Wu, W., & Malkawi, A. (2020). Optimization of Wind Positions for Wind-Driven Natural Ventilation Performance. *Energies*, *13*(10), 2464.

Moere, Fuller. Environmental Control Systems: Heating, Cooling, Lighting. McGraw-Hill College, 1992.

Chiang, C., Chen, N., Chou, P., Li, Y., & Lien, I. (2005, September). A study on the influence of horizontal louvers on natural ventilation in a dwelling unit. In *Proceeding of the 10th International Conference on Indoor Air Quality and Climate* (pp. 4-9).

Scheuring, L., & Weller, B. (2020). Natural ventilation provided by a self-sufficient facade system. In *IOP Conference Series: Earth and Environmental Science* (Vol. 410, No. 1, p. 012116). IOP Publishing.

Yang, Y. K., Kim, M. Y., Song, Y. W., Choi, S. H., & Park, J. C. (2020). Windcatcher Louvers to Improve Ventilation Efficiency. *Energies*, *13*(17), 4459.

Fritsch, R., Kohler, A., Nygård-Ferguson, M., & Scartezzini, J. L. (1990). A stochastic model of user behaviour regarding ventilation. *Building and Environment*, *25*(2), 173-181.

Yun, G. Y., Steemers, K., & Baker, N. (2008). Natural ventilation in practice: linking facade design, thermal performance, occupant perception and control. *Building Research & Information*, *36*(6), 608-624.

Chen, Y., Tong, Z., Samuelson, H., Wu, W., & Malkawi, A. (2019). Realizing natural ventilation potential through window control: the impact of occupant behavior. *Energy Procedia*, *158*, 3215-3221.